



# NI 43-101 TECHNICAL REPORT

on the Pucarini Property,  
in Distrito de Palca, Provincia  
de Lampa, Departamento de Puno. Juliaca,  
in Peru

15°55'56"S 70°30'51"W

For Forte Minerals Corp.

by  
Derrick Strickland, P. Geo.  
Steven Park, CPG  
Effective Date:  
February 15 2021

## Table of Contents

1	SUMMARY .....	4
2	INTRODUCTION.....	6
	2.1 Units and Measurements .....	7
3	RELIANCE ON OTHER EXPERTS .....	8
4	PROPERTY DESCRIPTION AND LOCATION.....	8
	4.1 Mineral Rights .....	11
	Overview of Mining Law .....	12
5	ACCESSIBILITY, CLIMATE, LOCAL RESOURCES, INFRASTRUCTURE AND PHYSIOGRAPHY	
	14	
6	HISTORY .....	15
7	GEOLOGICAL SETTING AND MINERALIZATION.....	15
	7.1 Regional Geology.....	15
	7.2 Property Geology .....	18
	7.2.1 Lithology .....	18
	7.2.2 Hydrothermal Alteration Facies.....	19
	7.2.3 Structure.....	20
	7.3 Hydrothermal Alteration and Mineralization .....	23
	7.4 Hydrothermal Alteration Facies.....	23
	7.4.1 Silicic (SIL) .....	23
	7.4.2 Argillic (ARG) .....	24
	7.4.3 Advanced Argillic (ADV).....	25
	7.5 Hydrothermal Breccia.....	25
8	DEPOSIT TYPES.....	27
	8.1 High-sulphidation Epithermal Precious Metal Deposits .....	27
	8.2 Classification of Sulphidation State.....	29
9	EXPLORATION.....	30
	9.1 Geologic Mapping .....	30
	9.2 Geochemistry .....	30
	9.2.1 Rock Chip Sampling.....	30
	9.2.2 Soil Sampling .....	32
	9.3 Geophysics .....	34
10	DRILLING.....	40
11	SAMPLING PREPARATION, ANALYSES, AND SECURITY.....	40
	11.1 Rock Chip Sampling.....	40
	11.2 Soil Sampling .....	40
	11.3 Stream Sediment Sample .....	41
	11.4 Spectral Analysis.....	41
12	DATA VERIFICATION .....	42
13	MINERAL PROCESSING AND METALLURGICAL TESTING.....	45
14	MINERAL RESOURCE ESTIMATE.....	45
15	THROUGH 22 ARE NOT APPLICABLE TO THIS REPORT .....	45
23	ADJACENT PROPERTIES.....	45
24	OTHER RELEVANT DATA AND INFORMATION .....	46
25	INTERPRETATION AND CONCLUSIONS.....	47
26	RECOMMENDATIONS.....	49
27	REFERENCES.....	51
28	CERTIFICATE OF QUALIFIED PERSON: .....	58

## LIST OF FIGURES

FIGURE 1: REGIONAL LOCATION MAP .....	9
FIGURE 2: PROPERTY MAP .....	10
FIGURE 3: GEOLOGIC, GEOPHYSICAL, AND TOPOGRAPHIC FEATURES.....	16
FIGURE 4: CORRELATION OF NEOGENE VOLCANIC UNITS .....	17
FIGURE 5. REGIONAL GEOLOGY AND MINERAL OCCURRENCES, CENTRAL SECTOR, DEPARTMENT OF PUNO.....	17
FIGURE 6: PYROCLASTIC ANDESITE .....	21
FIGURE 8: COLUMNAR JOINTS .....	21
FIGURE 9: PROPERTY GEOLOGIC MAP - LITHOLOGY.....	22
FIGURE 10: ALTERATION MAPPING .....	24
FIGURE 11: DARK, PLANAR RIBS OF SILICA-REPLACED ANDESITE PYROCLASTIC UNITS .....	25
FIGURE 12: SCHEMATIC SECTION A-B.....	26
FIGURE 13: SECTION THROUGH CHAQUICOCHA SUR DEPOSIT, YANACOCCHA .....	28
FIGURE 14: GOLD GEOCHEMISTRY IN ROCK CHIP SAMPLES FROM OUTCROP.....	31
FIGURE 15: GOLD AND ARSENIC GEOCHEMISTRY IN SOIL SAMPLES .....	33
FIGURE 16: CHARGEABILITY PLOTTED AT 150M BELOW SURFACE.....	36
FIGURE 17: INVERTED RESISTIVITY AND CHARGEABILITY SECTIONS FROM L7000. ....	36
FIGURE 18: MAP OF TOTAL MAGNETIC FIELD OUTLINING ZONES OF STRONG, MODERATE, AND WEAK DEMAGNETIZATION .....	39
FIGURE 19: OUTCROP SAMPLING IN THE ALTERED ZONE. ....	43
FIGURE 20: STEVE PARK ON THE NORTH RIDGE.....	43
FIGURE 21: CLOSE-UP OF SOIL SAMPLE SITE, LINE 7200 .....	43
FIGURE 22: CLOSED SAMPLE BAG WITH SAMPLE TICKET SECURED IN PLACE.....	43
FIGURE 23: ROCK MARKER WITH RED FLAGGING INDICATING A POINT ON GEOPHYSICAL LINE.....	43
FIGURE 24. MAP OF MINING CONCESSIONS ADJACENT TO AND NEAR THE PROPERTY.....	46
FIGURE 25: MAP SHOWING A SUMMARY OF KEY EXPLORATION TARGETING EVIDENCE .....	48

**LIST OF TABLES**

TABLE 1: DEFINITIONS, ABBREVIATIONS, AND CONVERSIONS .....	7
TABLE 2: DIAGNOSTIC MINERALS AND TEXTURES OF VARIOUS STATES OF PH.....	29
TABLE 3: AUTHOR SAMPLE COLLECTION NOTES .....	44
TABLE 4: SELECT AUTHOR CHECK ASSAYS.....	44
TABLE 5: PROPOSED BUDGET FOR DDH DRILL PROGRAM.....	49

## 1 SUMMARY

This report was commissioned by Forte Minerals Corp. (“Forte” or the “Company” and prepared by Derrick Strickland, P. Geo and Steven Park, CPG. As independent professional geoscientists, the authors undertook a review of available data, and were asked to recommend, if warranted, specific areas for further work on the Pucarini Property (or the “Property”). initial public offering of the Company on the Canadian Securities Exchange.

The Property consists of a single 1,000 ha (GBT-92) centred at 70° 30’ 51” W; 15° 55’ 56” S. The concession was acquired by Globetrotters Resources Peru SAC (“Globetrotters”) in 2018 and is currently held by Cordillera Resources SAC, a 99.99% owned subsidiary of Forte.

The Pucarini Property is an early-stage high-sulphidation gold project located approximately 43 km west-northwest of the city of Juliaca in the Department of Puno, Peru. The property was mapped and sampled by Teck Resources Peru SAC in the period 2011-2015, and subsequently dropped without having been tested by drilling. Globetrotters Resources Peru SAC acquired the property through the Peruvian auction process in 2018. Geological mapping and outcrop sampling were undertaken by Globetrotters in 2018 and 2019. The property was indirectly acquired by Forte under a share purchase agreement between Forte and Globetrotters Resources Group Inc. dated July 27, 2020 for the sale of, among other things, 459,739 shares of Cordillera Resource S.A.C. after which Forte continued exploration work by completing magnetometer, induced polarization, resistivity, and soil surveys.

The Property is in the Neogene magmatic arc of Southern Peru near the eastern margin of the Inner-Cordillera Occidental (Clark et al., 1990 and Sandeman et al., 1995). The Neogene magmatic arc formed on deformed Paleozoic and Mesozoic rocks, which are probably underlain by Neoproterozoic crystalline basement (Clark et al., 1990,). The Neogene magmatic arc is part of the persistent emplacement of intrusive and volcanic rocks throughout the Andean Orogeny that began in the very latest Triassic along the western margin of South America (McKee and Noble, 1989; Pitcher, 1985; and Stewart et al., 1974). Relatively short episodes of active volcanism separated by periods of volcanic quiescence lasting up to 25 Ma. during construction of the main arc continued through the Neogene.

The Company conducted an exploration program on the Pucarini Project from October 26 to November 17, 2020. The program included a geochemical survey concurrent with geologic mapping followed by a geophysical survey. A total of 124 rock samples, 552 soil samples, and one stream sediment sample were collected during the geochemical survey. The geophysical survey consisted of 27.55 line-km of induced polarization (IP) and 82.31 line-km of ground magnetics that were oriented following the results of the geochemical survey and geologic mapping.

The volcanic sequence on the Property was intensely altered by hydrothermal fluids that produced hypogene alunite, pyrophyllite, quartz (silica) and jarosite, a mineral assemblage that defines advanced argillic type of alteration as commonly found in high-sulphidation gold systems.

Alteration mapped by the Company shows strong silica-dominant alteration enveloped by broader clay-dominant alteration. Kaolinite is the dominant clay phase in the argillic alteration zone. Dickite has been identified from spectral analysis. Advanced argillic mineral assemblages consisting of hydrothermal alunite, pyrophyllite, white mica, and diaspore accompany silica replacement. Silica replacement zones define northwest, north, and northeast oriented fractures in the volcanic succession. Faulting in the Property area has not been resolved.

Induced Polarization (IP) geophysical survey lines were positioned over the strongest mineralization and alteration as recognized from preceding surface mapping and geochemical sampling programs. Domains of reduced magnetic susceptibility correspond well with the extensive zone of argillic alteration that destroys primary magnetite found in the local andesite and dacite volcanic units. The type of hydrothermal alteration observed on the Property is magnetite-destructive and causes a reduction in magnetic susceptibility. Relatively weak alteration observed at surface in areas of low magnetic susceptibility suggest that hydrothermal alteration is more intense at depth.

Four exploration targets that were established by geological mapping, geochemical sampling, and geophysical surveys require drilling as the next step in testing for gold mineralization. An initial program of drilling is recommended to test these targets with 1,000 metres of core drilling for an estimated cost of CAD\$689,972.

## 2 INTRODUCTION

This report was commissioned by Forte Copper Corp. (Forte or the Company) and prepared by Derrick Strickland, P. Geo. and Steven Park, CPG. As independent professional geoscientists, the authors undertook a review of available data, and were asked to recommend, if warranted, specific areas for further work on the Pucarini Property (or the “Property”). initial public offering of the Company on the Canadian Securities Exchange.

The authors are “qualified persons” within the meaning of National Instrument 43-101. This report is intended to be filed with the Securities Commissions in all the provinces of Canada except for Quebec.

In the preparation of this report, the authors utilized information provided by the Company as well as technical reports that have been previously published on [www.sedar.com](http://www.sedar.com). Results for the historical exploration on the Property is discussed in Section 6 of this report. A list of reports, maps, and other information examined by the authors is provided in Section 27 of this report.

This technical report is based on the following sources of information:

- Discussions with Forte Minerals Corp.
- Current Personal Inspection of the Pucarini Property
- Review of geological data provided by Globetrotters Resource Group Inc.
- Additional information obtained from public domain sources

The authors reserve the right, but will not be obliged, to revise the report and conclusions if additional information becomes known subsequent to the date of this report.

As of the date of this report, the authors are not aware of any material fact or material change with respect to the subject matter of this technical report that is not presented herein, or which the omission to disclose could make this report misleading.

Steven Park, CPG, undertook a site visit on November 22, 2020, during which time he reviewed the geological setting and collected six verification samples on the Property. Mr. Park is responsible for sections 7, 8, 10 and 12 of this report. Derrick Strickland P. Geo. has not visited the Property. Unless otherwise stated, the maps in this report were created by Derrick Strickland, P. Geo. Mr. Strickland is responsible for sections 1 to 6, 9, 11, 13 to 27 of this report.

## 2.1 Units and Measurements

Table 1: Definitions, Abbreviations, and Conversions

Abbreviation	Meaning	Abbreviation	Meaning
'	Feet = 30.48 cm	kg	kilogram(s)
"	Inch =2.54 cm	km	kilometer(s)
%	Percentage	m	meter(s)
%	percent(age)	Ma	million years
USD	United States Dollars	masl.	Meters Above Sea Level
<	less than	mg	milligram(s)
>	greater than	mile	5 280 ft= 1.609344 km
°	degree(s)	QC	quality control
°C	degrees Celsius	NI 43-101	Canadian National Instrument 43-101
1 gram	0.3215 troy oz	mm	millimeter(s)
1 oz/Ton	28.22 gm/tonne	Mudstone	A sedimentary rock composed predominantly of clay and silt
1 troy oz	31.104 gm	n.a.	not available/applicable
Anomaly	An area highlighted by a geochemical or geophysical survey as possessing greater than background metal values or physical characteristics	Mineralization	The process or processes by which mineral or minerals are introduced into a rock, resulting in a valuable or potentially valuable deposit
asl	above sea level	Outcrop	An exposure of bedrock at the surface
Au	Gold	Ag	Silver
Basin	A depressed sediment filled area	Permian	The period of geological time between about 251 and 298 million years ago
Bedrock	Solid Rock underlying surficial deposits	opt	Ounce per tone
Cenozoic	The era of geological time from the present to about 65 million years ago	ppb	parts per billion
Chalcopyrite	A sulphide mineral of copper and iron; the most important ore mineral of copper.	ppm	Parts per million (same as grams per tonne)
Chip sample	A method of sampling a rock exposure whereby a regular series of small chips of rock is broken off along a line across the face, back or wall.	Proterozoic	The eon of geological time between about 545 and 2,500 million years ago
cm	centimeter(s)	QA	quality assurance
Conglomerate	A very coarse-grained sedimentary rock containing rounded to subangular pebbles, cobbles, and / or boulders set in a finer grained matrix	Mineral	A naturally occurring homogeneous substance having definite physical properties and chemical composition and, if formed under favorable conditions, a definite crystal form.
DDH	diamond drill hole	Quartz	A mineral composed of silicon dioxide
Disseminated	A rock texture comprised of randomly scattered minerals (usually crystalline) throughout the rock mass	Sandstone	A sedimentary rock composed primarily of sand sized grains
		Sediment	A particulate matter that has been transported by fluid flow, potentially creating a sedimentary rock unit
EM	Electromagnetic Geophysical Survey	Shale	A fine-grained detrital sedimentary rock formed from clay and silt
Epithermal	Hydrothermal mineral deposit formed within one kilometre of the earth's surface, in the temperature range of 50–200°C.	Siltstone	A fine-grained detrital sedimentary rock formed predominantly of silt
Epithermal deposit	A mineral deposit consisting of veins and replacement bodies, usually in volcanic or sedimentary rocks, containing precious metals or, more rarely, base metals.	Stratigraphy	Composition, sequence and correlation of stratified rock in the earth's crust
Exploration	Prospecting, sampling, mapping, diamond drilling and other work involved in searching for ore.	Sulphides	A group of minerals which contains sulphur and other metallic elements such as copper and zinc. Gold is usually associated with sulphide enrichment in mineral deposits.
Fault	A fracture in rock along which there has been relative displacement	Supergroup	A formally named assemblage of related sedimentary groups
Fe	Iron	T	ton (2000 pounds or 977.2 kg)
Feldspars	A group of rock-forming tectosilicate minerals, (KAlSi3O8 - NaAlSi3O8 - CaAl2Si2O8)	t	tonne (1000 kg or 2,204.6 pounds)
Float	loose pieces rock on the surface not outcrop	VLF-EM	Very Low Frequency Electro Magnetic Geophysical Survey
g or gm	gram(s)	W	Tungstine
g/t	grams per metric tonne	Zn	Zinc
Galena	Lead sulphide, the most common ore mineral of lead	GPS	Global Positioning System
IP	Induced Polarization Geophysical survey	ha	hectare(s)

### **3 RELIANCE ON OTHER EXPERTS**

The authors have relied upon a legal opinion on mineral title dated November 27th 2020 written by Mario Chirinos Dongo of Dentons Gallo Barrios Pickmann SCRL with address of General Cordova N0 313 Miraflores, Lima 18 Peru. This legal opinion is detailed in Section 4 of this report.

### **4 PROPERTY DESCRIPTION AND LOCATION**

The Pucarini Property (the “Property”) is located in southeastern Peru in the District of Palca, Province of Lampa, Department of Puno. The city of Juliaca, the region’s largest commercial centre, is 43 km from the Property with a driving time of approximately 1 hour (Figure 1). Juliaca is located 830 km southeast of Lima.

The Property consists of a single mining concession of 1,000 hectares and named GBT-92 and centred at 70° 30’ 51” W; 15° 55’ 56” S (Figure 2). This concession was acquired by Globetrotters Resources Peru SAC (“Globetrotters”) in 2018 and is currently held by Cordillera Resources SAC, a 99.99% owned subsidiary of Forte.

A legal opinion dated November 27, 2020 written by Mario Chirinos Dongo of *Dentons Gallo Barrios Pickmann SCRL*, with address of General Cordova N0 313 Miraflores, Lima 18 Peru was provided to the authors. The legal opinion addressed mining rights on the Property stating that Cordillera Resources SAC is the exclusive and unique title holder of the concession GBT-92. Also noted is a 1% NSR Royalty granted to Globetrotters Resources Peru SAC. The legal opinion confirms that Cordillera Resources SAC is a Peruvian Subsidiary of the Company.

Pursuant to a share purchase agreement dated July 27, 2020 between Globetrotters Resource Group Inc and Forte, Forte acquired the Peruvian companies Cordillera Resources SAC and Amaru Resources SAC for aggregate consideration of 5,000,000 shares and CAD\$150,000 in cash payment to Globetrotters Resource Group Inc. Several other Peruvian mineral concessions held by Globetrotters are also included in the July 27, 2020 agreement (shown in Figure 1). The subject of this technical report is only mineral concession GBT-92.



Figure 1: Regional Location Map

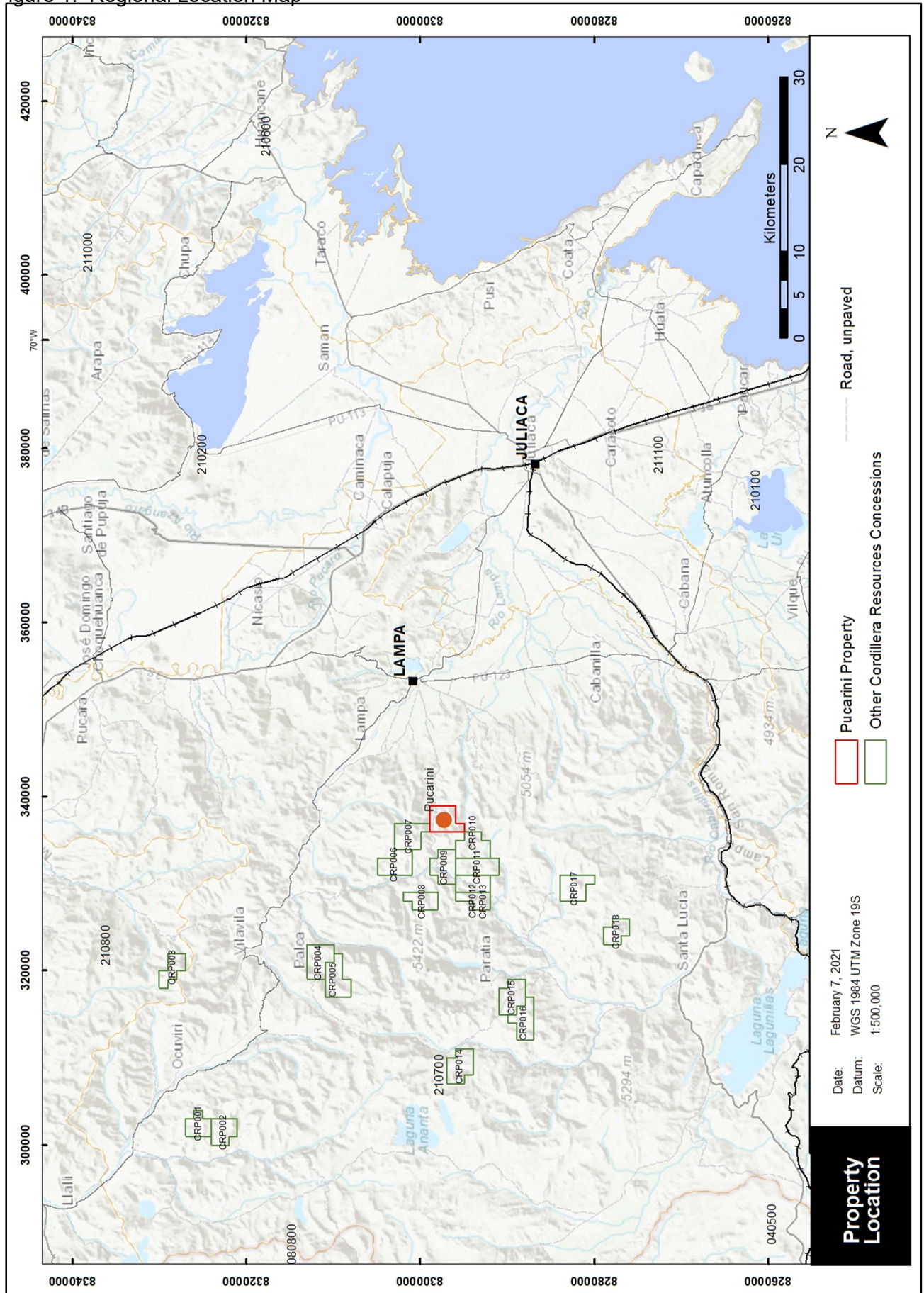
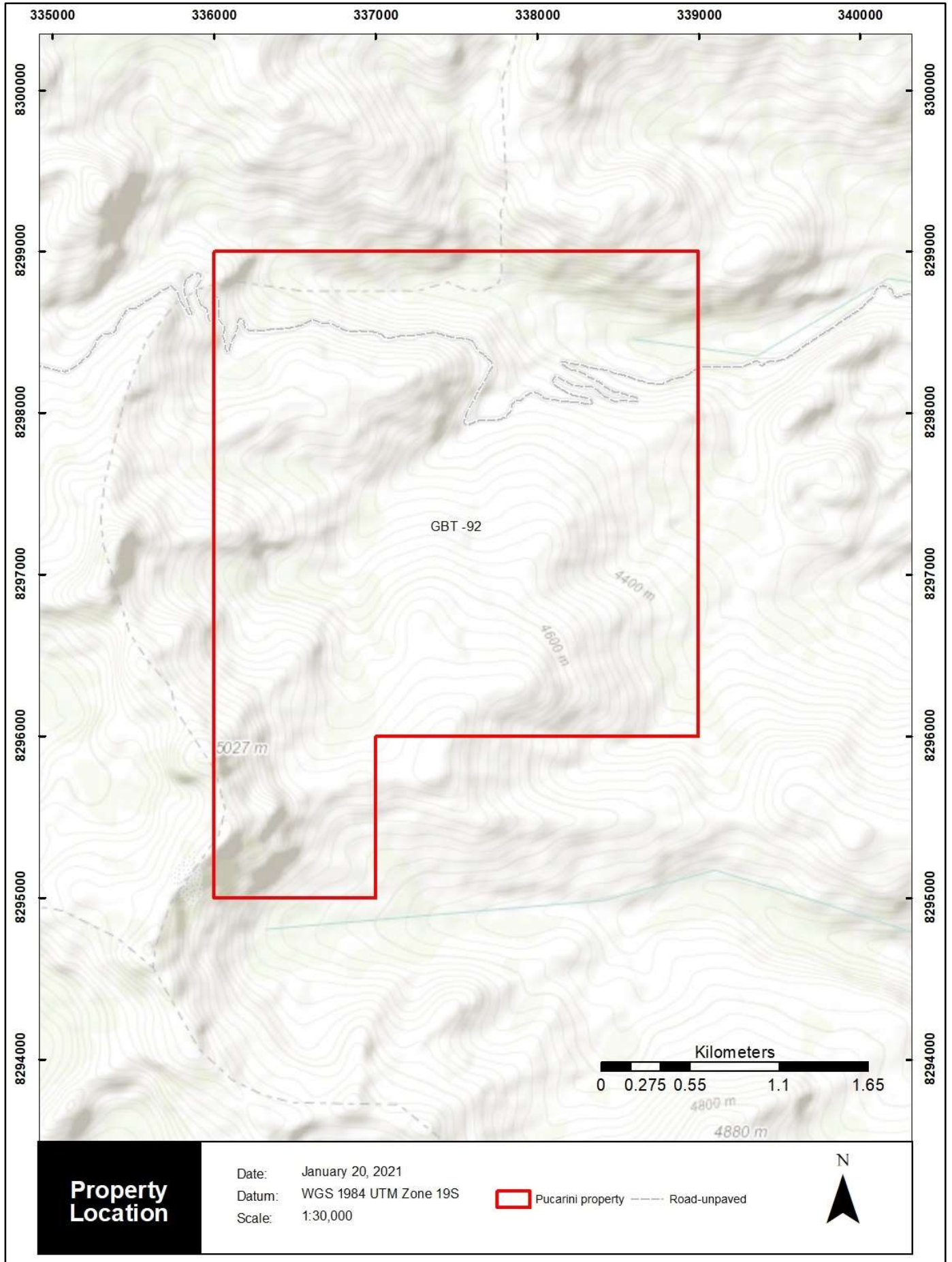


Figure 2: Property Map



## 4.1 Mineral Rights

The General Mining Law of Peru defines and regulates different stages of mining activities ranging from sampling and prospecting, to development, mining, and processing. The General Mining Law of Peru was changed in the mid-1990's to foster the development of the country's mineral resources. The law further defines and regulates different categories of mining activities according to the stage of development (prospecting, exploitation, processing, and marketing). The Peruvian State does not have free carry rights or options to acquire shareholdings in mining companies. There are no requirements for participation in ownership of mining rights by indigenous persons, groups or entities.

Titles over mineral claims are controlled by the Institute of Geology, Mining and Metallurgy ("INGEMMET"). The current status of any mining right can be verified by accessing INGEMMET's nationwide online concessions database at <https://geocatmin.ingemmet.gob.pe/geocatmin/>. Mining concessions in Peru are valid for both exploration and mining activities. There is no discrimination between local and foreign ownership of the concessions unless the mining concession is within 50 km of the Peru border. Titles to mining concessions are granted using map datum UTM WGS 84 coordinates (Law No. 30428); prior to 2017 coordinates were listed using map datum UTM PSAD 1956. New mining concessions must be at least of 100 ha in size (1 km<sup>2</sup>) and must be oriented in a north-south or east-west direction. Pre-existing concessions, based on the old system (known as "Punto de Partida" or the starting point system), were located in any orientation and did not have a minimum size requirement.

The Mining Grid System corresponds to the 1:100,000 scale National Chart grid drawn up by the National Geographic Institute in the system WGS84, and defines areas whose vertices are located with UTM coordinates expressed in whole kilometres, based on of a grid of one kilometre on each side, equivalent to 100 hectares, as a minimum extension of the claim or concession.

All holders are required to move into production in due time and meet the thresholds for Minimum Annual Production ("MAP") or investment levels. If MAP or required investment are not made after year 10, the holder would have to pay a penalty equivalent to 2% of the minimum production<sup>1</sup>, currently estimated at approximately US\$26.00 per hectare. MAP is defined as a single tax unit (Unidad Impositiva Tributaria, "UIT"), equivalent to approximately US\$1,300.00. These rates apply to large and medium scale producers, while small scale and artisanal miners benefit from lower thresholds (i.e., 5-10% of the UIT for small-scale producers and 5% for artisanal miners).

If the threshold for minimum production is not reached after 10<sup>th</sup> year, the penalty increases up to 5% of the MAP (appr. ~US\$65.00 per hectare) required per year from the 15<sup>th</sup> year and to 10% of MAP (appr. US\$130.00 per hectare) from the 20<sup>th</sup> year.

---

<sup>1</sup> In accordance with the provisions of article 40 of General Peruvian Mining Law, approved by Supreme Decree No. 014-92-EM, modified by Legislative Decree N° 1320.

## 4.2 Overview of Mining Law

*Ministerio de Energía y Minas de Peru* (the Ministry of Energy and Mines of Peru) is the principal central government body in Peru responsible for regulating and managing the energy and mining sectors. Mining activities are defined and regulated through the General Mining Law of Peru, approved by the Peruvian Congress in 1992. Reconnaissance, prospecting, exploration, exploitation (mining), general labour, beneficiation, commercialization, mineral transport, and mineral storage outside a mining facility are the mining activities defined under the General Mining Law. Mining concessions are granted to local and foreign individuals or legal entities by *Ministerio de Energía y Minas de Peru* (“MINEM”) through the Institute of Geology, Mining and Metallurgy (“INGEMMET”). INGEMMET is responsible for issuing mining concessions, maintaining a register of all issued mining concessions, and administering all taxes, payments and penalties related to issued mining concessions. Geological surveys and research are also conducted by INGEMMET.

Authorization to begin exploration and mining activities is issued by a section of MINEM known as the General Directorate of Mining (“DGM”). DGM also issues permits for general labour, beneficiation, and mineral transport activities as defined under the General Mining Law. The Mining Industry is also subject to the Prior Consultation Law, which defines the public consultation process for projects that may have an impact on indigenous people. The process must be conducted before project approval is granted.

Environmental compliance of all mining projects is governed by the Agency for Environmental Assessment and Inspection (“OEFA”), an agency of the Ministry of the Environment (*Ministerio del Ambiente*). OEFA governs evaluation, supervision, inspection, and sanction of environmental matters pertaining to mining projects and operations. Environmental certifications for projects that require a semi-detailed Environmental Impact Assessment (“EIASd”) are issued by the Environmental Certification National Service (“SENACE”) of the Ministry of the Environment.

### Environmental Regulations & Exploration Permits

The General Mining Law, administered by the Ministry of Energy and Mines (“MEM”), may require a mining company to prepare an Environmental Evaluation (“EA”), an Environmental Impact Assessment (“EIA”), a Program for Environmental Management and Adjustment (“PAMA”), and a Closure Plan prior to mining construction and operation.

The Supreme Decree N° 020-2004-EM classifies the environmental requirements for mining and exploration programs as follows:

- **Category I:** This category includes mining projects involving small-scale drilling programs up to and including a maximum 40 drill pads, a disturbed area of fewer than 10 hectares considering drilling platforms, trenches, auxiliary facilities and access means or the construction of tunnels with a total maximum length of 50 metres. These projects require the preparation of an Environmental Impact Declaration (“*Declaración de Impacto Ambiental*” or DÍA). Category I permits require, before their submittal to the Ministry of Energy and Mines, water-use permits from the Ministry of Agriculture, if required, and land-use agreements with the surface rights owners in the form of a registered agreement resulting from town-hall meetings in the local community(s).

- **Category II:** This category includes mining projects involving more than 40 drill pads, a disturbed area of more than 10 hectares considering drilling platforms, trenches, auxiliary facilities and access, or the construction of tunnels over a total length of 50 metres, require an authorisation called an Environmental Impact Study-semi detailed (“Estudio de Impacto Ambiental-semi detallado” or “EIA-sd”) and is approved by the Ministry of Energy and Mines. Category II permits, which include mining projects involving more than just drilling, must include, before their submittal to the Ministry of Energy and Mines, water-use permits from the Ministry of Agriculture, land-use agreements with the surface rights owners and evidence of having held town-hall meetings in all nearby communities. Additionally, the EIA-sd must include a detailed reclamation program once the drilling phase ends.

No permit is required for surface exploration such as surface mapping, sampling or geophysics. Permission of the surface rights owner is required for access to the property and for any surface disturbance such as trenching or the construction of trails.

According to Paul Johnston (P. Geo.) of Globetrotters, the Company is in the process of acquiring all the information to submit a DIA to the Peruvian Government.

### **Royalties and Obligations**

Peru established a sliding scale of mining royalties in 2004, later modified in 2011. The modified mining royalties are the greater of 1% of sales or 1-12% applied to operating income.

The following is a summary of the main taxes that apply to miners in Peru (in addition to the annual holding fees of \$0.50-\$3.00/Ha):

- Corporate tax rate is 29.5%;
- Dividend withholding tax is 5%;
- Special Mining Tax of 2% to 8.4% applied to operating mining income; and
- Special Mining Burden of 4% to 13.12% applied to operating income (only applies to mining companies with tax stabilization agreements prior to 2011); and 8% of net profit paid to employees.

Foreign investors and local enterprises may apply for particular tax, currency and other stability agreements with the government of Peru, provided that specific requirements and minimum investments are met. The agreements guarantee stability for a term of ten years concerning: (i) the income tax regime; (ii) the currency exchange regime, including the free availability of foreign currency and free remittance of capital and profits abroad (only for foreign investors); and (iii) non-discrimination.

## **5 ACCESSIBILITY, CLIMATE, LOCAL RESOURCES, INFRASTRUCTURE AND PHYSIOGRAPHY**

The Property is located 43 km west-northwest of the city of Juliaca, the closest full-service city and the largest city in the Department of Puno. Regularly scheduled commercial flight service is available from the Juliaca airport to Lima and other major airports throughout Peru. Access to the Property is by unpaved, maintained public roads from Lampa, which is the closest town located 16 km to the east of the Property. Lampa is connected to Juliaca and Arequipa by the national highway network.

Pucarini has a temperate climate with a wet season from October through March and a dry season from April to September. Temperatures average 8.8°C (0.7 to 17.4°C) in the wet season and 6.2°C (-4.4 to 15.8°C) in the dry season. Precipitation averages 88.0 mm during the wet season and 14.5 mm during the dry season. Snow is common in August through November at higher elevations. The property topography ranges between 4,300 and 4,700 m above mean sea level.

Area vegetation is dominated by grass and small shrubs. Plants become increasingly sparse with higher elevations. The Property is characterized by moderate slopes and local steep slopes adjacent to drainages. An unpaved public road maintained by local communities transects the northern edge of the property and connects smaller populated places with Lampa, the nearest town to the Property.

## **6 HISTORY**

The only evidence of prospecting activity is a small prospect shaft located near the southern boundary of the Property. Teck Resources Peru SAC explored the area in 2011-2015 and, according to informal verbal accounts, completed geological, geochemical, and geophysical surveys but exploration records are unavailable. The Property became available for staking when Teck relinquished the ground in 2017.

Globetrotters successfully acquired the property through the regular bidding process in 2018. Globetrotters staff completed reconnaissance style mapping and sampling during 22 days of field exploration from 2018 to 2019 with objectives to outline the extent of hydrothermal alteration, characterise alteration style, and determine mineralization controls through geochemical surveys and spectral analysis of alteration minerals. The geochemical analysis was completed on 90 rock chip samples; 333 samples comprised of outcrop chips were analyzed by high-resolution mineral spectrometer (Terra Spec).

## **7 GEOLOGICAL SETTING AND MINERALIZATION**

### **7.1 Regional Geology**

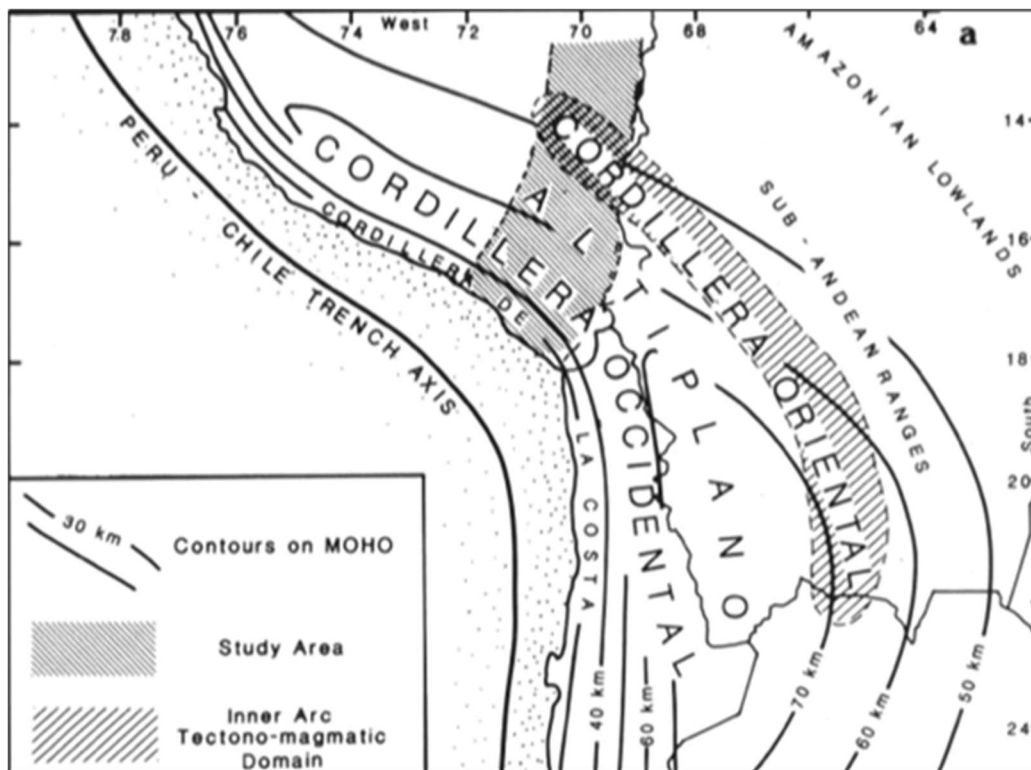
The Property resides in the Neogene magmatic arc of Southern Peru near the eastern margin of the Inner-Cordillera Occidental (Clark et al., 1990, and Sandeman et al., 1995) as denoted in Figure 3 and Figure 4. The Neogene magmatic arc formed on deformed Paleozoic and Mesozoic rocks, which are probably underlain by Neoproterozoic crystalline basement (Clark et al., 1990). The Neogene magmatic arc is part of the persistent emplacement of intrusive and volcanic rocks throughout the Andean Orogeny that began in the very latest Triassic along the western margin of South America (McKee and Noble, 1989; Pitcher, 1985; Stewart et al., 1974). Relatively short episodes of active volcanism were separated by periods of volcanic quiescence lasting up to 25 Ma during construction of the main arc continuing through the Neogene.

The volcanic succession in the Pucarini area consists of andesite to dacite lava and pyroclastic units of the Miocene Sillapaca Formation dated 8.0 – 16.9 Ma (McKee and Noble, 1989, and Jenks, 1946) which appears to be similar to the volcanic units hosting the Arasi gold mine located 25 km to the northwest. The Quechua II unconformity (8 Ma) separates the Sillapaca volcanics from the Late Miocene to Pliocene Barroso Group (Benavides-Cáceres, 1999). Early Miocene volcanic rocks of the Tacaza Group have not been recognized in the immediate area of the project but appear on regional geology maps. Similarly, late Miocene to Pliocene, mainly acidic volcanic rocks equivalent to the Sencca Group, and younger andesitic lava flows related to Pliocene volcanoes assigned to the Barroso Group dated 5.6 – 6.7 Ma (Palacios Moncayo et al., 1993) do not occur in the project area (Figure 5).

The Late Cretaceous marks a time of a major tectonic and magmatic shift throughout the Andes coincident with the opening of the south Atlantic Ocean (Tosdal, 2003). Generally, there is migration of arc development towards the northeast. In southern Peru, the time is marked by Late Cretaceous shortening, collapse of the back-arc rift and eastward thrusting of marine volcanic

and sedimentary sequences on top of continentally derived clastic rocks (Vicente et al., 1989, and Benavides-Cáceres, 1999). Magmatism continued in central and southern Peru during the Late Cretaceous (66 Ma) and continued into Paleogene time (59 Ma) (Clark et al., 1990) and is responsible for obscuring the earlier rift sequence and late Cretaceous fold and thrust belt. This arc is preserved as thick dacitic to andesitic pyroclastic rocks and intermediate flows (Bellido, 1979) with igneous roots composed of large, Proterozoic-aged granodiorite batholiths derived from mantle and lower crustal material (Barreiro and Clark, 1984; and Boiley et al., 1990). This period of magmatism is correlative with the Toquepala Group rocks in the area between Toquepala and Cuajone (as seen in Figure 4).

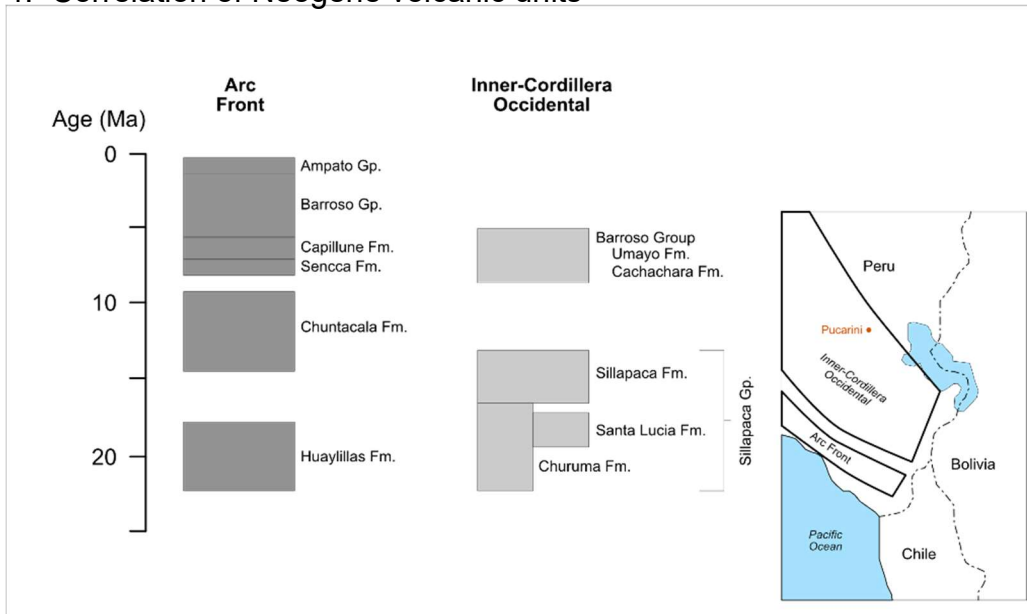
Figure 3: Geologic, geophysical, and topographic features



Geologic, geophysical, and topographic features of the central Andes in the vicinity of the Arica deflection (southern Peru, northern Chile, and western Bolivia) from Clark et al. (1990) showing major physiographic provinces with contours of crustal thickness. The Altiplano and Cordillera Occidental correspond with the entire Main Arc, which consists of the Inner Arc and Inner-Cordillera Occidental.

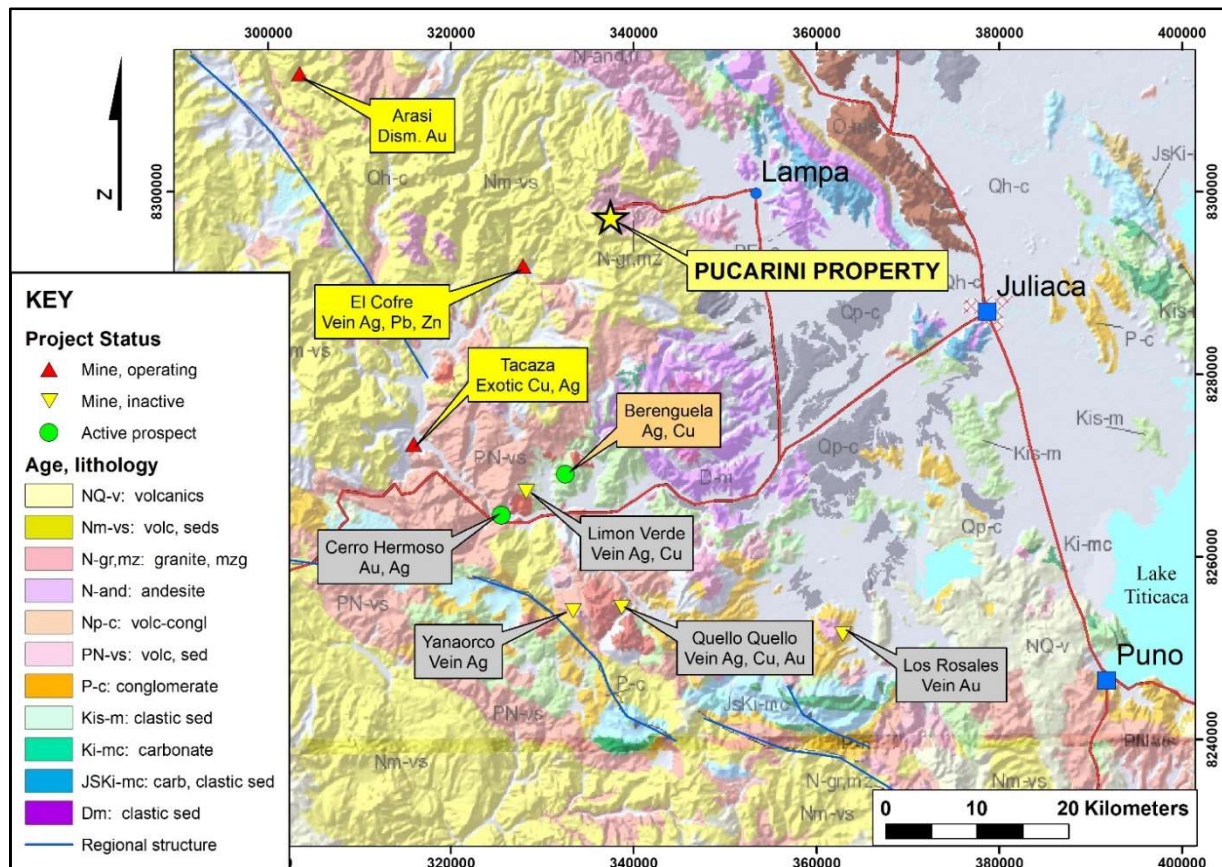


Figure 4: Correlation of Neogene volcanic units



Correlation of Neogene volcanic units in the Arc Front and Inner-Cordillera Occidental parts of the Main Arc in southern Peru. Modified after Sandeman et al. (1995)

Figure 5. Regional geology and mineral occurrences, central sector, Department of Puno



## 7.2 Property Geology

Host rocks for gold mineralization on the Property are tentatively assigned to the Miocene-age Sillapaca Formation. The Sillapaca Formation is a volcanic succession dominated by thickly stratified andesite pyroclastics and lava with lesser dacite pyroclastic layers (Figure 6). Figure 9 is the mapped geology on the Property illustrating the spatial relationships of the units described below.

### 7.2.1 Lithology

#### **Quaternary Colluvium (Q-col)**

Unconsolidated colluvium. Poorly sorted gravel, sand, and silt with lesser angular blocks derived from weathering and breakdown of underlying rock. Widespread deposits on hillslopes as sheetwash, rain-wash, or downslope transport.

#### **Quaternary Alluvium (Q-al)**

Unconsolidated alluvium composed of gravel, sand, and silt. Deposited by a stream or other non-marine body of running water as a sorted or semi-sorted sediment in the bed of the stream, or in the stream's floodplain or delta. Also as a cone or fan at the base of a slope.

#### **Quaternary Consolidated Colluvium (Q-mo)**

Consolidated, poorly sorted angular blocks, gravel, sand, and silt derived from weathering and breakdown of underlying rock. Restricted deposits on hillslopes as sheetwash, rain-wash, or downslope transport.

#### **Miocene Rhyolite (N1-rhy)**

Rhyolite flow. Light grey, fine-grained to aphanitic massive lava.

#### **Miocene Dacite (N1-dac)**

Fine-grained to aphanitic grey groundmass. Phenocrysts in the porphyritic textured variety consist of 1-3 mm diameter quartz (5% vol.), 1-4 mm length plagioclase phenocrysts (20-35% vol.), 1-3 mm diameter black biotite (1-5% vol.), and minor fine-grained hornblende. Dacite flows occur as light-coloured, narrow, volumetrically minor discontinuous layers. The presence of quartz phenocrysts distinguishes this unit from andesite.

#### **Miocene Dacite Tuff (N1-dtuf)**

Dacite tuff. Light purple-brown ash groundmass with <10% lapilli, 2-8mm length broken and intact plagioclase crystals (10-25% vol.), 1-2 mm diameter subrounded quartz crystals (2-5% vol.), 1-4 mm diameter black biotite (5% vol.) and minor, very fine-grained hornblende.

#### **Miocene Dacite lapilli tuff (N1-dltuf)**

Light purple-brown ash groundmass with 40-50% lapilli. Phenocryst content is identical to the dacite tuff (above). Lapilli are of the same composition as the ash. Accidental clasts are rare. Lapilli are elongated or flattened; welding is common.

### **Miocene Andesite Flow (N1-and)**

Purple grey. Not differentiated by texture. Very fine-grained to aphanitic groundmass. Porphyritic variety has 2-8 mm length plagioclase phenocrysts, (10-25% vol.), and 0.5-3.0 mm length hornblende (5% vol.) set in a fine grained, dark grey, slightly purple or brown aphanitic or very fine-grained groundmass. Amygdules have not been observed. Andesite forms 0.5 - 50m thick layers in the volcanic succession. Columnar jointing is common in thicker layers (Figure 8).

### **Miocene Andesite Flow, Aphanitic Texture (N1-anda)**

Andesite flow. Grey, very fine-grained to aphanitic massive lava. Fine-grained plagioclase and hornblende may be visible. Vesicles or amygdules have not been observed. Andesite forms 0.5 - 50m thick layers in the volcanic succession. Columnar jointing is developed in thicker layers.

### **Miocene Andesite Flow, Porphyritic Texture (N1-andp)**

Andesite flow. 2-8 mm length plagioclase phenocrysts (10-25% vol.) set in a fine-grained dark grey, slightly purple or brown aphanitic or very fine-grained groundmass. 0.5-3.0 mm length hornblende (5% vol.). Amygdules have not been observed. Andesite forms 0.5 to 50 m thick layers in the volcanic succession. Columnar jointing is common in thicker layers.

### **Miocene Andesite Tuff (N1-atuf)**

Andesite tuff is composed of >90% volcanic ash containing abundant broken plagioclase crystals. It is deposited in 0.1 – 1.0 m thick layers normally as minor interlayers with andesite lapilli tuff. Welding of pyroclastic material is common. Hornblende and biotite are the mafic constituents.

### **Miocene Andesite Lapilli Tuff (N1-altuf)**

Andesite lapilli tuff is composed of 70-90% ash with 2-5 cm diameter juvenile andesite fragments (10-30% vol.). Variably broken plagioclase crystals make up to 25% of the ash component. Lapilli clasts are flattened with welding common in most exposures. Andesite lapilli tuff unit accounts for the largest volume in the volcanic succession (Figure 7).

### **Miocene Andesite Lapilli Tuff, Welded (N1-altufw)**

Andesite lapilli tuff as above (N1-altuf) but with flattened lapilli clasts and welded pyroclastic components.

### **Miocene Andesite Volcanic Breccia (N1-avbx)**

Large (>64 mm), block-size angular to sub-rounded clasts of andesite cemented with fine-grained to aphanitic andesite. Brecciation is the result of internal processes acting during movement of semisolid or solid lava (e.g. autoclastic).

## **7.2.2 Hydrothermal Alteration Facies**

Three main hydrothermal alteration facies are defined for mapping purposes based on the alteration mineral assemblages present. Minerals characteristic of the alteration facies are

recognisable with a hand lens. Field observations are supported by spectral analysis samples collected from outcrops.

### **Silicic (SIL)**

Silica replaces felsic sites, fine-grained groundmass, and introduced as open space filling. Silica may also result as a residual product of strong leaching by acidic hydrothermal solutions. Different styles of silica alteration, such as vuggy and steam heated silica have not been differentiated at the present level of mapping.

### **Advanced Argillic (ADV)**

Hydrothermal alunite, pyrophyllite, and diaspore are commonly observed. Hydrothermal alunite has a crystalline texture that is easily distinguished with a hand lens. Crystal masses typically appear with a pale pink color. Pyrophyllite occurs as very fine-grained, clear crystal aggregates with a pearly lustre. White mica may be detected or recorded as sericite.

### **Argillic (ARG)**

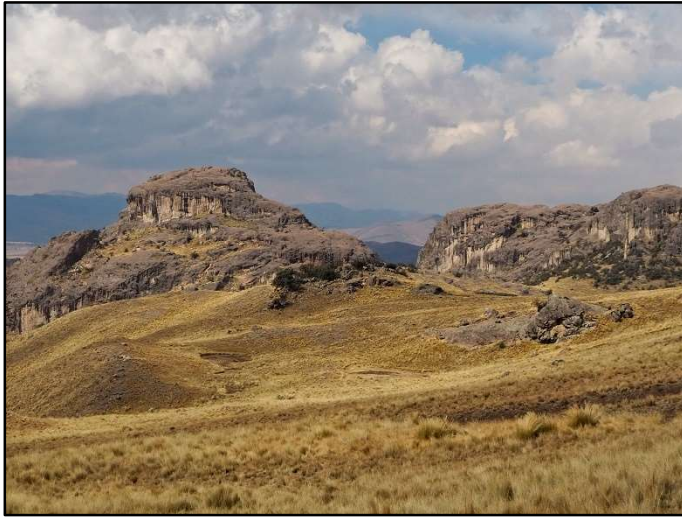
Clay minerals replace felsic and mafic sites. Kaolinite is the most common alteration mineral. Smectite and dickite are identified from spectral analysis. Alteration intensity is classified based on the amount or degree of replacement at felsic sites.

## **7.2.3 Structure**

Recognition of the structural grain across the Property by surface mapping has been limited by the scarcity of outcrop. The outcrops that have remained, however, are resistant to erosion primarily due to their higher content of silica introduced along structural conduits – faults and fractures - during hydrothermal alteration processes. Field mapping shows that these outcrops are primarily oriented with strike directions to the northwest following the regional Andean structural trend with minor conjugate structures trending to the east or northeast.

The most prominent of these structural trends on the Property extends along irregular exposures more than 2,500 m in a northwest strike direction (Figure 10). Shorter trends of outcrops (approximately 500 m in length) are found in sub-parallel trends to the south of the primary structure. The alteration map defines short, discontinuous linear outcrops of advanced argillic alteration striking to the northeast, intersecting with the primary NW structural trend.

Figure 6: Pyroclastic andesite



Thick, horizontal pyroclastic andesite belonging to the Miocene-age Sillapaca Formation. The exposures shown are outside the alteration zone present on the Property.

Figure 7: Unaltered andesite



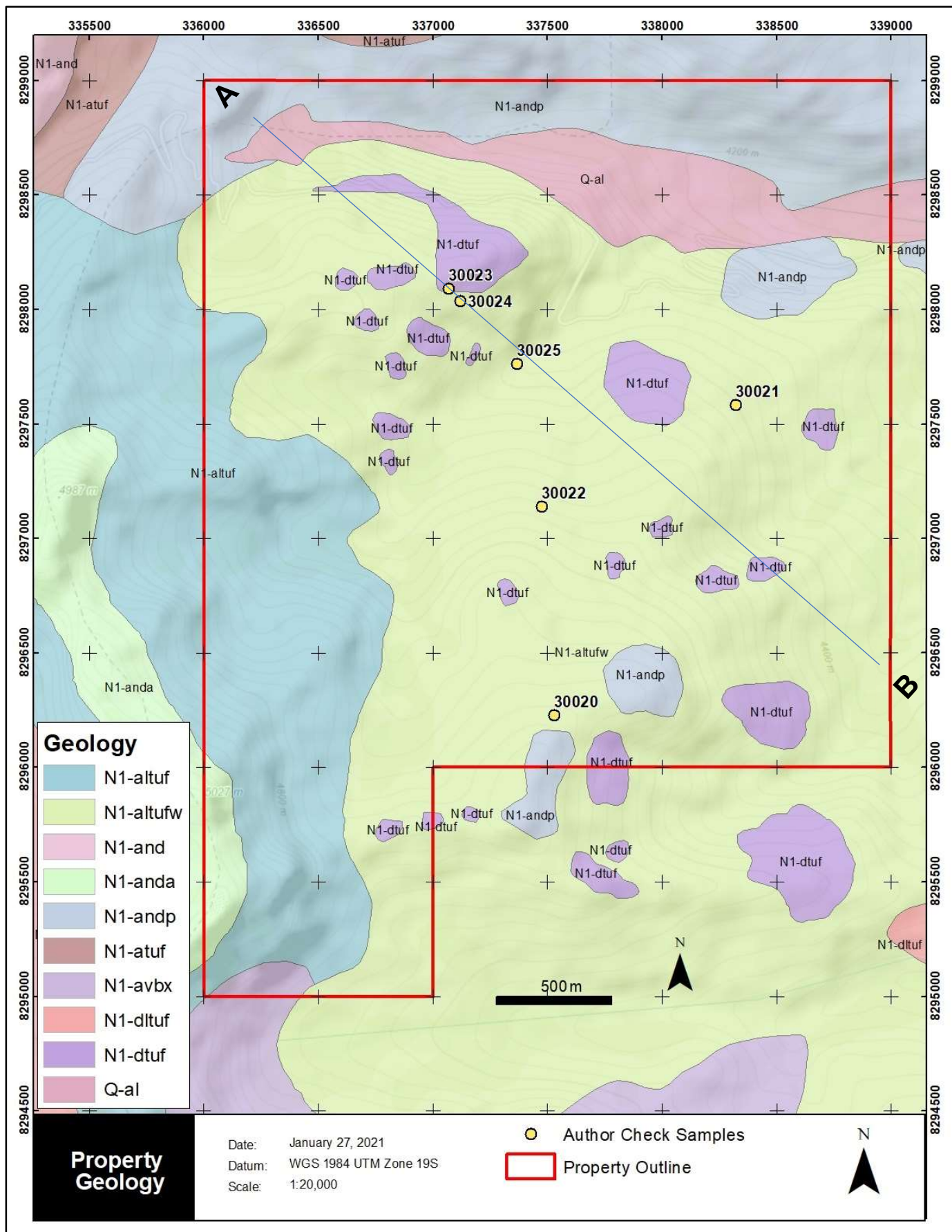
Example of unaltered andesite lapilli tuff. Variably broken plagioclase crystals and lapilli are common and reveal the pyroclastic character. Plagioclase crystals have obvious cleavage and are glassy. Lapilli are visible in the centre and top-centre of the sample. Unaltered andesite has distinctive purple-brown matrix.

Figure 8: Columnar joints



Columnar joints developed in horizontal, well-layered and weakly altered andesite flows. Individual layers are 50-200 cm thick. This exposure is on the outer limit of the mapped Pucarini alteration zone. Minor white clay (kaolinite) incipiently replaces primary plagioclase and also occurs along some fracture surfaces where it is accompanied by jarosite. Minor chlorite partially replaces mafic sites in the andesite and traces of epidote replace plagioclase. Field relationships show peripheral propylitic alteration overprinted by argillic alteration.

Figure 9: Property Geologic Map - Lithology (Section A-B shown in Figure 12)



### **7.3 Hydrothermal Alteration and Mineralization**

The volcanic sequence on the Property was intensely altered by hydrothermal fluids that produced hypogene alunite, pyrophyllite, quartz (silica) and jarosite, a mineral assemblage that defines advanced argillic type of alteration as commonly found in high-sulphidation gold systems. Outcrop mapping and geochemical sampling supported by spectral analysis of rock chips outlined two main subparallel alteration/mineralization trends (Figure 10).

Light brown, orange, and yellow colours related to argillic alteration in contrast with dark grey, unaltered andesite allow alteration zones to be confidently delimited by both remote sensing techniques and field mapping. Alteration and mineralization are controlled by a complex array of mineralized, steeply dipping fractures distributed across the property. The fracture arrays are enclosed by broader argillic alteration zones with alteration gradients decreasing outward to propylitically altered andesite. Kaolinite, alunite, illite (white mica), and pyrophyllite are alteration phases recognised in the field visually with the aid of a hand lens and confirmed by spectral analysis. Diaspore, paragonite, and dickite have been identified by spectral analysis of outcrop rock chips.

Fractures and faults control the distribution of alteration at all scales. Hydrothermal quartz is present as quartz veins and cement to hydrothermal breccias that occur in the fractures, and as pervasive replacement of wall rock adjacent to the fractures. Jarosite after pyrite commonly accompanies quartz veins and breccia. Wall rock adjacent to veins and fractures contains kaolinite, white mica (sericite and/or illite), alunite, and quartz with less common pyrophyllite, dickite and diaspore. Outboard of the silica-dominated alteration, hydrothermal kaolinite replaces felsic and mafic sites with diminishing intensity away from the fractures or veins. An alteration pattern is apparent at a property scale in which an irregular, linear zone of quartz veining and brecciation extending NW-SE over 2,500 meters is marked by an alteration assemblage of silica-kaolinite-alunite-white mica ± pyrophyllite and an outer envelope of kaolinite-dominant alteration as illustrated in Figure 11.

### **7.4 Hydrothermal Alteration Facies**

Three hydrothermal alteration facies are defined for mapping purposes based on the alteration mineral assemblages present. Minerals characteristic of each alteration facies are recognisable in the field with a hand lens. Field observations are supported by spectral analysis of hand samples collected from outcrops (Figure 10).

#### **7.4.1 Silicic (SIL)**

Silicic alteration is characterized by silica replacement in felsic sites and fine-grained groundmass, and as open space filling. Silica may also result as a residual product of strong leaching by acidic hydrothermal solutions. Different styles of silicic alteration, such as vuggy and steam heated silica, have not been differentiated at the present level of mapping. Silica replacement zones define northwest, north, and northeast oriented fractures in the volcanic succession.

## 7.4.2 Argillic (ARG)

Clay minerals replace felsic and mafic sites. Kaolinite is the most common alteration mineral. Smectite and dickite are identified from spectral analysis. Alteration intensity is classified based on the amount or degree of replacement at felsic sites.

The alteration map for the Pucarini property shows strong, silica-dominant alteration enveloped by broader clay-dominant alteration. Kaolinite is the dominant clay phase in the argillic alteration zone. Dickite has been identified from spectral analysis.

Figure 10: Property Geologic Map - Alteration

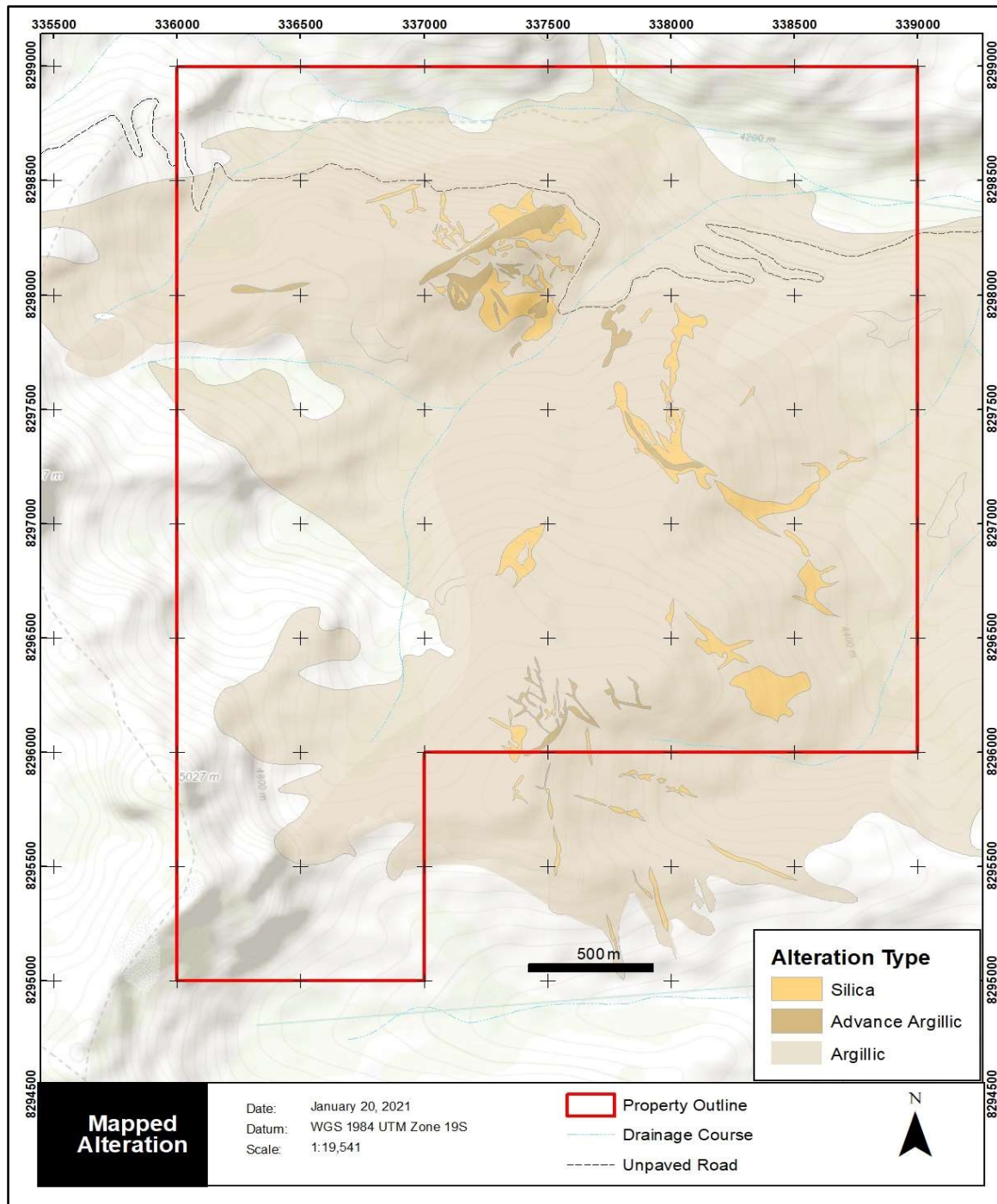




Figure 11: Dark, planar ribs of silica-replaced andesite pyroclastic units



Dark, planar ribs of silica-replaced andesite pyroclastic units enclosed by strong clay alteration accompanied by jarosite exposed on hillsides. A tabular, sub-vertical silica-rich rib with abundant yellow jarosite is visible in the foreground. Multiple orientations of fracture-controlled silica ribs are evident in the photograph. Abundant jarosite is associated with the rib of silica replacement in the foreground and has a strike oblique to the photograph. Multiple orientations of silica ribs are visible on the hillside. Alunite, white mica and less common pyrophyllite are present with the silica. Unaltered, horizontal layers of andesite are visible in the upper left corner of the photograph (After Globetrotters 2021)

### 7.4.3 Advanced Argillic (ADV)

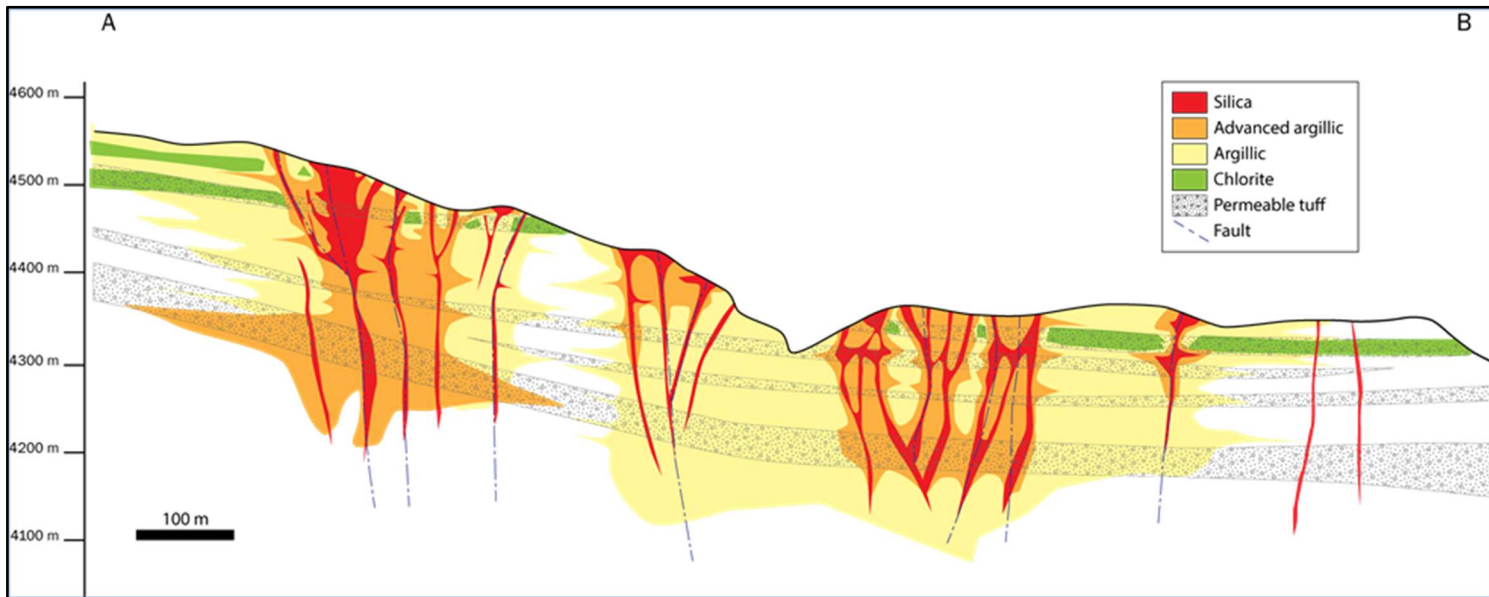
Advanced argillic mineral assemblages consisting of hydrothermal alunite, pyrophyllite, white mica, and diaspore accompany silica replacement. Hydrothermal alunite is easily distinguished with a hand lens as pale-pink, coarse crystalline masses. Pyrophyllite occurs as very fine-grained, clear crystalline aggregates with a pearly lustre. White mica may be detected or recorded as sericite. Diaspore has been reported from spectral analysis.

### 7.5 Hydrothermal Breccia

Hydrothermal breccia occurs in tabular, vertical structures described in the preceding section as breccia dikes and veins. In addition, larger hydrothermal breccia bodies with pipe-like geometry have plan dimensions in the order of 50-100 metres and irregular shapes. They are associated with the more intense clay alteration. Mapping has not progressed sufficiently to accurately delimit any individual, large hydrothermal breccia bodies.

Figure 12 is a schematic section illustrating alteration controls on the Property. The exploration hypothesis involves hydrothermal fluid transmitted along vertical fractures that cut the horizontal volcanic sequence and control alteration and mineralization. Horizontal mineralized zones are inferred where conduits intersect permeable volcanic layers. Extensive argillic alteration encloses more restricted advanced argillic alteration associated with silica and gold mineralization.

Figure 12: Schematic Section A-B



See Figure 9 for the location of "A" and "B" (modified from Globetrotters, 2021). View to the northeast

## **8 DEPOSIT TYPES**

### **8.1 High-sulphidation Epithermal Precious Metal Deposits**

The character of alteration and gold mineralization on the Pucarini Property is consistent with high-sulphidation epithermal precious metal deposits. Hedenquist (1987) proposed the term high-sulphidation to classify epithermal deposits originating from low pH (acid) hydrothermal fluids exsolved from magma bodies emplaced at shallow crustal levels. The distinctive alteration and potential ore minerals associated with this deposit class reflect the acidic nature of hydrothermal fluids involved in their formation. Well-known examples of high-sulphidation gold deposits are: Yanacocha, Peru (Harvey et al., 1999; Teal and Benavides, 2010); Pierina, Peru (Rainbow et al., 2005); Pueblo Viejo, Dominican Republic (Nelson, 2000); El Indio, Chile (Jannas et al., 1990); Comstock, USA (Hudson, 2003); Tonopah, USA (Sillitoe and Hedenquist, 2003); and Lepanto, Philippines (Hedenquist et al., 1998).

The diverse size, grade, depth and geometry of epithermal precious and base metal deposits is a function of different tectonic, igneous, and structural settings where they occur and the multiple mineralization and alteration processes involved in their formation (White and Hedenquist, 1990). Most high-sulphidation epithermal deposits are concentrated along convergent plate margins in coeval or slightly older volcanic units of calc-alkalic affinity. A smaller proportion of this deposit type are hosted in the basement rocks underlying the volcanic units (Sawkins, 1990). The largest proportion of deposits are Cenozoic because of their poor preservation potential. Deposit formation in areas of high-relief and rapid uplift erode quickly. Although much less common, older examples occur such as the Mesozoic Cerro Vanguardia deposit in Argentina (Schalamuk et al., 1997).

Principal factors influencing the character of mineralization are geology, chemistry of hydrothermal fluid, pressure, temperature, and hydrology. Faulting and fracturing, host rock stratigraphy, and intrusions determine deposit geometry. Metal transport, ore mineralogy, vein composition, alteration assemblages and alteration intensity are influenced by hydrothermal fluid chemistry. Hydrothermal fluid flow is governed by primary and hydrothermally induced permeability of host rock units and fault/fracture arrays. These factors combine to influence the resultant size and grade of the mineral deposit (Sillitoe, 1993; Sillitoe and Hedenquist, 2003).

Mineralization commonly occurs in steeply dipping veins in association with minor faults showing small displacements or fractures. Examples of deposits hosted in major faults are uncommon. Strike lengths of these veins can be greater than 1,000 m; their vertical extent may range an order of magnitude from 10 to 100's of metres.

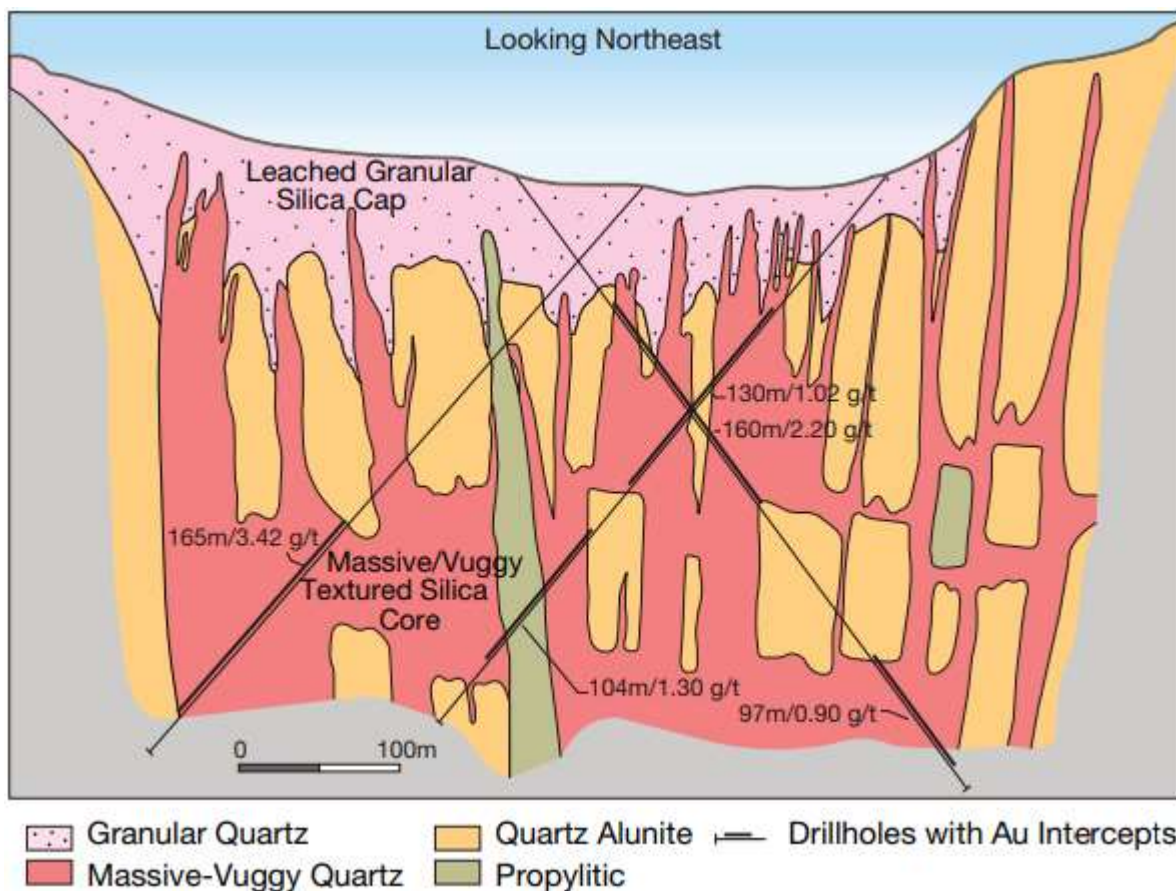
Quartz is the dominant gangue mineral in veins and associated wall-rock alteration. Pyrite is the dominant sulphide; its content is highly variable from trace amounts to >25 volume percent. Most high-sulphidation epithermal deposits are mined for gold and silver, but other metals such as copper and zinc have been recovered as significant credits with Au-Ag ore.

The Yanacocha gold system is a large, well-documented, high-sulphidation gold system located in northern Peru that exhibits classic advanced argillic alteration patterns. Gold mineralization is

hosted in a Miocene volcanic sequence composed of felsic and intermediate pyroclastic units and minor lava. Alteration is characterized by extensive silica replacement and residual silica related to hydrothermal leaching by acidic fluids. Alunite, kaolinite, pyrophyllite, and diaspore are the main alteration phases that are spatially associated with silica alteration and gold mineralization. Alteration is most intense along vertical hydrothermal fluid conduits of massive and vuggy silica enveloped by advanced argillic alteration (Figure 12).

The qualified person has not verified the information on the Yanacocha gold system and the information disclosed is not necessarily indicative of mineralization on the Property that is the subject of the technical report. Mineralization hosted on adjacent and/or nearby and/or geologically similar properties is not necessarily indicative of mineralization hosted on the Company's Property.

Figure 13: Section through Chaquicocha Sur deposit, Yanacocha



This section from Yanacocha illustrates the occurrence of gold in sub-vertical, massive/vuggy silica structures enveloped by advanced argillic alteration and capped by a leached zone of granular silica (Teal and Benavides, 2010).

## 8.2 Classification of Sulphidation State

Sulphidation, as used to distinguish the oxidation state of aqueous sulfur species in hydrothermal solutions (White and Hedenquist, 1990; Hedenquist and Lowenstern, 1994), was integrated with petrology studies to quantify stabilities of sulfur-bearing minerals on the basis of sulphur fugacity (Barton and Skinner, 1967, Hedenquist et al., 1994; Einaudi et al., 2003) to characterize low-, intermediate-, and high-sulphidation states. Einaudi et al. (2003) recognized that the sulphidation state of ore-forming fluids varied through time and space and that the variability in sulfide species, especially Cu-, Fe-, and As-bearing sulfides, was in response to processes within an evolving hydrothermal environment.

The simple approach of Hedenquist (1987) using fundamental fluid chemistry appears to be the most practical method as the fluid chemistry can be readily inferred from vein and alteration mineralogy, alteration zoning, and deposit form determined from field observation. In applying this approach, it is important to establish mineral paragenesis for identifying minerals that form with mineralization and not include minerals that predate and post-date mineralization. A growing body of research shows early, highly reactive hydrothermal fluid responsible for intense rock leaching evolves to a more reduced (intermediate) fluid, which may be responsible for mineralization (Stoffregen, 1987). The evolution of hydrothermal fluid composition is probably related to increased mixing of magmatic and meteoric water (Giggenbach, 1988). Diagnostic minerals of the three most commonly used classification schemes are summarized in Table 2. The obvious correlation of acid pH alteration style with high-sulphidation sulfide mineral assemblage causes informal interchange of the two classification schemes.

Table 2: Diagnostic Minerals and Textures of Various States of pH

<b>Acid pH</b>	<b>Neutral pH</b>	
Alunite, kaolinite (dickite), pyrophyllite, residual/vuggy quartz	Quartz-adularia ± illite, calcite	
<i>High sulphidation</i> Pyrite-enargite, ± luzonite, covellite, digenite, famatinite, orpiment	<i>Intermediate sulphidation</i> Tennantite, tetrahedrite, hematite-pyrite, magnetite, pyrite, chalcopyrite, Fe-poor sphalerite-pyrite	<i>Low sulphidation</i> Arsenopyrite-loellingite-pyrrhotite, pyrrhotite, Fe-rich sphalerite-pyrite
<i>Oxidized</i> Alunite, hematite-magnetite	<i>Reduced</i> Magnetite-pyrite-pyrrhotite, chlorite-pyrite	

Sulphidation and oxidation state used to distinguish epithermal ore-forming environments (Giggenbach, 1997; Einaudi et al., 2003). (The use of hyphens between minerals indicates an equilibrium assemblage for which all phases need to be present). From Simmons et al. (2005).

## **9 EXPLORATION**

The Company conducted an exploration program on the Pucarini Project from October 26 to November 17, 2020. The program included geochemical surveys concurrent with geologic mapping. A total of 124 rock samples, 552 soil samples, and one stream sediment sample were collected during the geochemical survey. The geophysical survey consisted of 27.55 line-km of induced polarization (IP) and 82.31 line-km of ground magnetics that were oriented following the results of the geochemical survey and geologic mapping.

### **9.1 Geologic Mapping**

All recent exploration work undertaken on the Property was conducted or controlled by Globetrotters. Exploration by Globetrotters was initiated with reconnaissance-style geological mapping and outcrop sampling of mineralized structures, primarily quartz veins and hydrothermal breccia dikes. Geological mapping outlined intense silica replacement, residual silica, advanced argillic, and argillic alteration zones focussed along two subparallel, west-northwest oriented alteration zones. Subsequent mapping has shown subsidiary advanced argillic alteration zones connect the two dominant zones and all are enclosed by a broad zone of argillic alteration. Propylitic alteration with a mineral assemblage of chlorite + epidote ± pyrite ± calcite surrounds the argillic alteration. Routine analysis of rock chips from outcrop by spectral methods confirms the mineral assemblages determined by field observations.

### **9.2 Geochemistry**

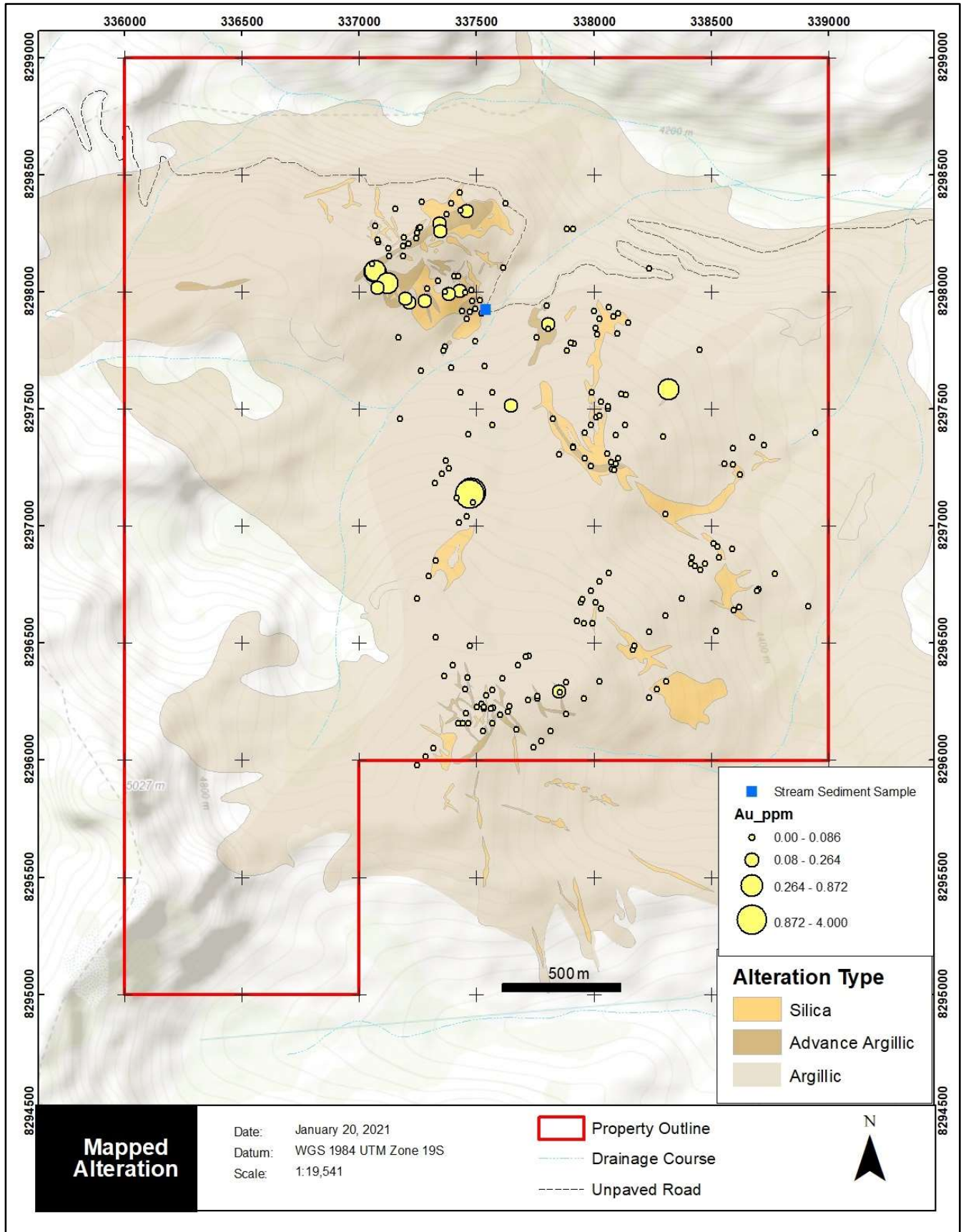
#### **9.2.1 Rock Chip Sampling**

Globetrotters personnel collected 124 samples from mineralized and altered outcrops. These samples indicate gold mineralization is associated with hydrothermal brecciated dikes and veins, and quartz veining associated with higher temperature alteration indicated by quartz-pyrophyllite. Broad zones of very fine-grained disseminated pyrite do not show a direct association with gold. More sampling is necessary to understand the controls and timing of gold deposition.

Most rock chip samples that returned gold values greater than 0.5 ppm Au were collected from outcrops at elevations lower than 4,500 m. Rock chip samples collected from veins and breccia dikes at higher elevations returned values <0.1 ppm Au. This observation suggests an elevation control on gold mineralization (Figure 14).

Outcrop sampling indicates gold is associated with hydrothermal breccia dikes and veins associated with higher temperature advanced argillic alteration assemblages containing pyrophyllite. More comprehensive outcrop sampling and mapping was completed in mid-November, 2020 leading to the observation that gold is associated with silica-dominated alteration occurring as hydrothermal cement in breccia dikes and pervasive replacement in wall rock of breccia dikes and quartz veins. Most quartz (silica) was introduced after clay-pyrite alteration as shown in rare outcrops located at lower elevations. Limited rock chip sampling indicates low gold grades in this early phase of alteration.

Figure 14: Gold geochemistry in rock chip samples from outcrop.



## 9.2.2 Soil Sampling

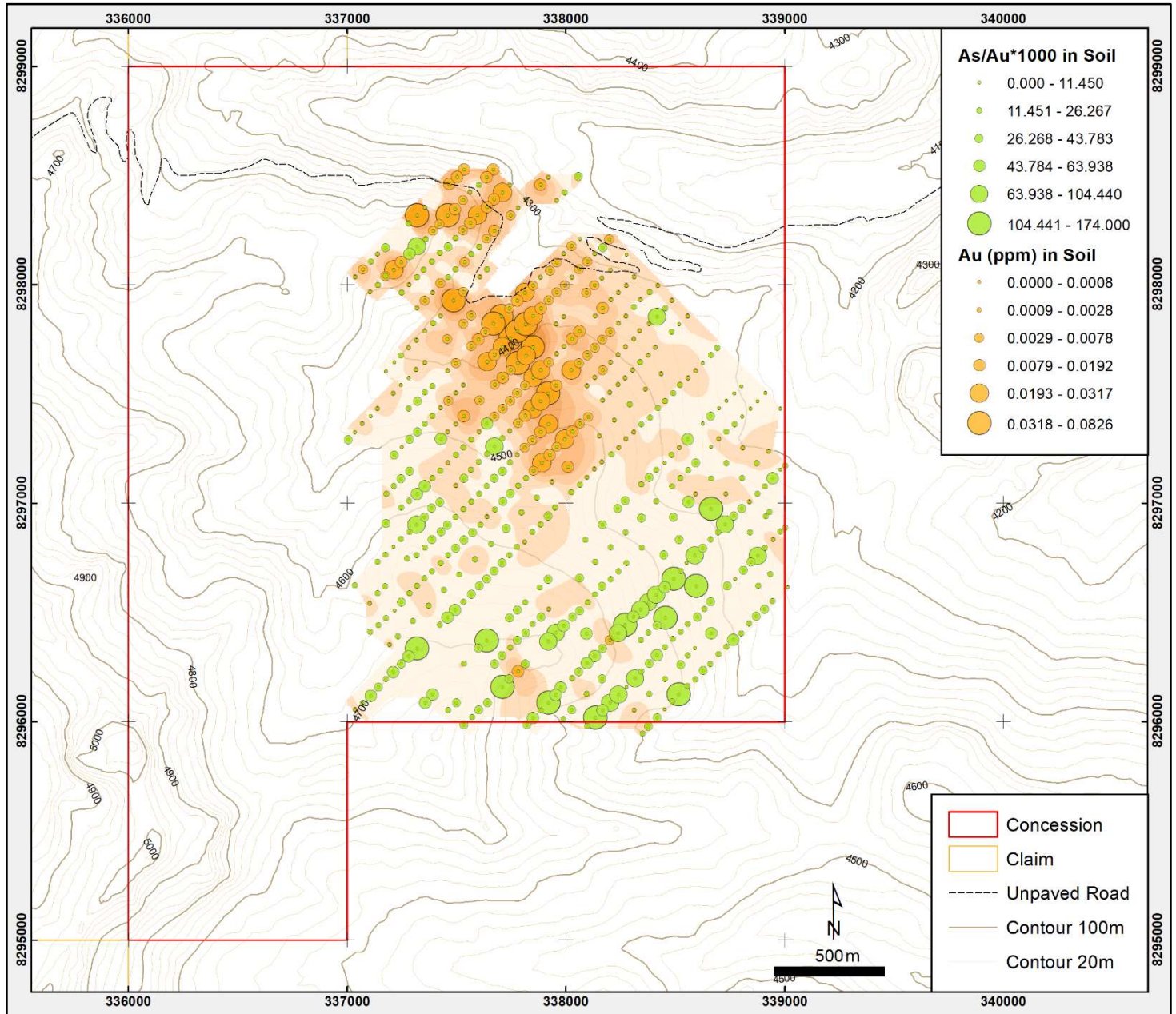
To date, 552 soils samples have been collected from the Property. The soil geochemical program was effective at identifying a coherent gold anomaly in soil above a bedrock source measuring 1.5 x 0.9 km (Figure 15). The soil anomaly coincides with anomalous outcrop samples and zones of high chargeability and high resistivity subsequently defined by the IP geophysical survey. The soil anomaly is open to the north and northwest. Higher arsenic values peripheral to the gold anomaly may reflect a temperature gradient established while the epithermal system was active causing arsenic, tellurium, and zinc to deposit outboard of gold, molybdenum, barium, and copper.

Arsenic, zinc, and tellurium anomalies on the fringes of the soil grid are both laterally and vertically above the gold. Limited outcrop and soil data indicate there is a vertical control on gold mineralization. The arsenic anomalies at higher elevations on the south side of the soil grid are significant in that they suggest gold mineralization occurs at depth and could connect to the gold anomaly to the north at a lower elevation.

Soil geochemical results show that gold anomalies in soil are localized around mineralized outcrops, including on the up-slope side, with minimal down-slope migration of the gold anomaly indicating that little dispersion of gold in soil has occurred. The soil anomalies suggest that gold mineralization is more extensive and continuous than inferred from the geochemical results from rock chip sampling.



Figure 15: Gold and arsenic geochemistry in soil samples



After Globetrotters 2021

### 9.3 Geophysics

Magnetometry and Induced Polarization (IP) surveys were planned for Q2-2020 but it was necessary to delay the work until late October 2020 due to travel restrictions arising from the global COVID-19 pandemic. The geophysical program comprising 27.55 line-km of IP (see Figure 16 for location) and 82.31 line-km of ground magnetic surveying (Figure 18 for grid location) was completed on November 22, 2020 by Deep Sounding E.I.R.L. (Deep Sounding).

The magnetometry survey was conducted with 2 crews simultaneously operating GEM Overhauser magnetometers. This type of magnetometer has a sensitivity of 0.022 nT at 1 Hz and a resolution of 0.01 nT. A differential GPS was used to position measurements. Surveying was conducted along north-oriented survey lines aligned parallel to the WGS84 zone19S UTM grid and spaced at 200 m. The survey results contain a noticeable amount of magnetic noise, which is attributed to higher-than-normal diurnal magnetic field fluctuations and the small distance between the magnetic sensor and ground surface. The noise produces high-frequency variations along survey lines that are especially noticeable on the east side of the survey grid.

The IP survey used a pole-dipole electrode array to measure chargeability and resistivity with a variable electrode spacing of 50, 100, 150, and 200 metres. Survey lines were spaced at 200 metre intervals on an azimuth of 045°. Survey stations were located using a differential GPS. Deep Sounding used a GDD Model GRx8-32-time domain IP receiver capable of reading up to 32 channels. The transmitter was a Walcer Geophysics Limited Hunttec KW10, which has 10 output voltage selections of 100 to 3,200 volts.

IP survey lines were positioned over the strongest mineralization and alteration as recognised from preceding surface mapping and geochemical sampling programs.

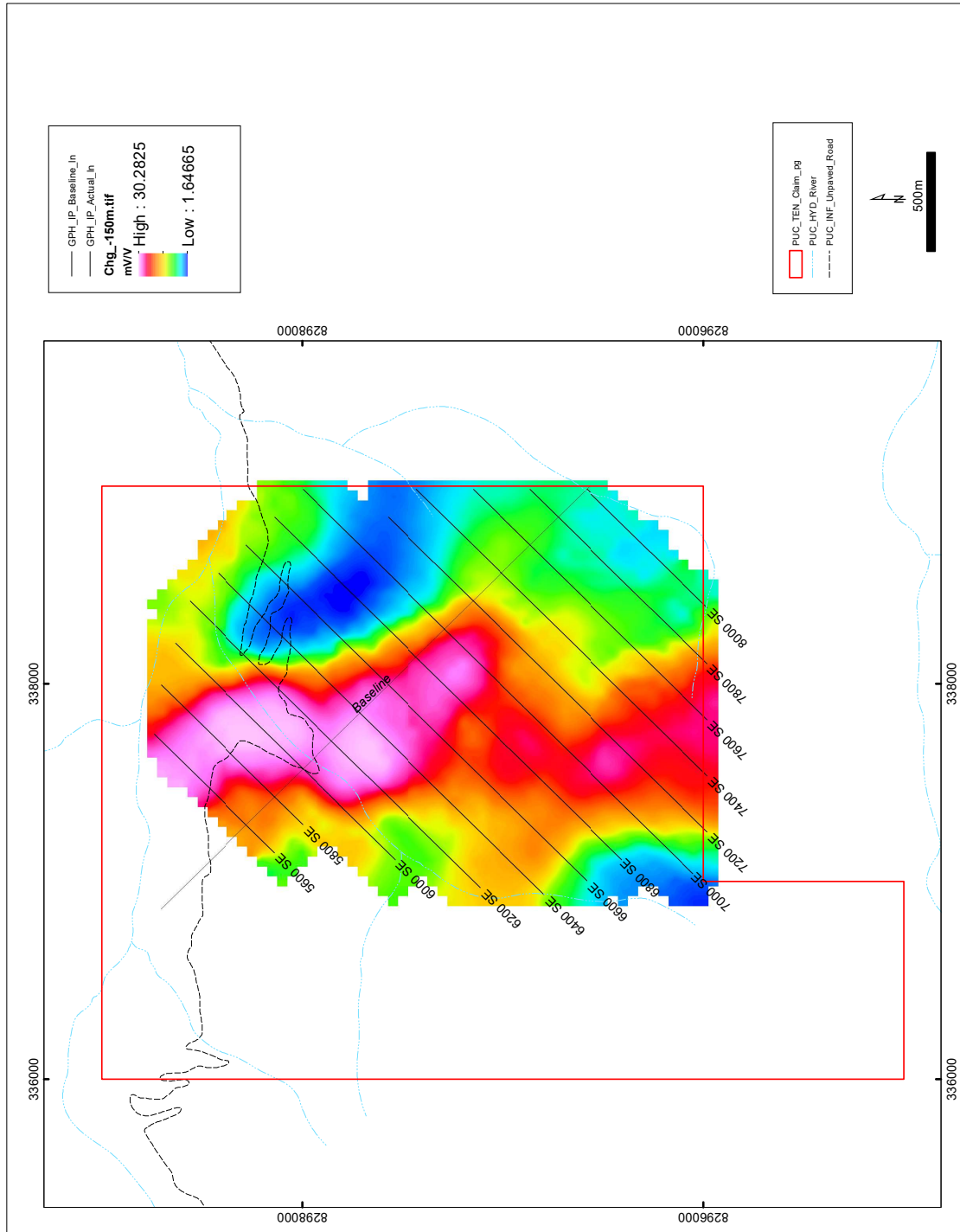
Total Field magnetic response is shown in Figure 17 with an inverted colour palette. The geomagnetic field is close to horizontal in this location and inverting the colour palette is a common technique for simulating a reduction to pole (RTP) filter. Magenta-coloured domains are unaltered andesite units.

Zones of high resistivity in the northern sector of the grid at lower elevations correlate with strong silica alteration (see Figure 16). The northwestern resistivity anomaly appears as a near-surface, flat feature on lines 5600 through 6200. The southeast resistivity anomaly forms a coherent zone on lines 6400 through 7200. It is more deeply seated with a vertical form compared with the northwest anomaly. A larger zone of high resistivity is located on the south side of the survey grid and is interpreted as silica alteration located beneath an array of narrow but persistent breccia dikes and breccia veins. This anomaly has a flat geometry near surface on lines 6400 to 7200 with a root appearing on lines 6600 to 7800 that persists to the lower limit of the inversion model. The two lobes of higher resistivity are located on the flanks of a prominent north-trending chargeability zone (Figure 16). The chargeability anomaly appears as a vertical feature on the inverted chargeability sections (Figure 17).

The main chargeability anomaly shows correlation with a deep conductive body caused by alteration associated with the formation of the deposit, an event that caused the formation of secondary porosity with the consequent drop in resistivity.

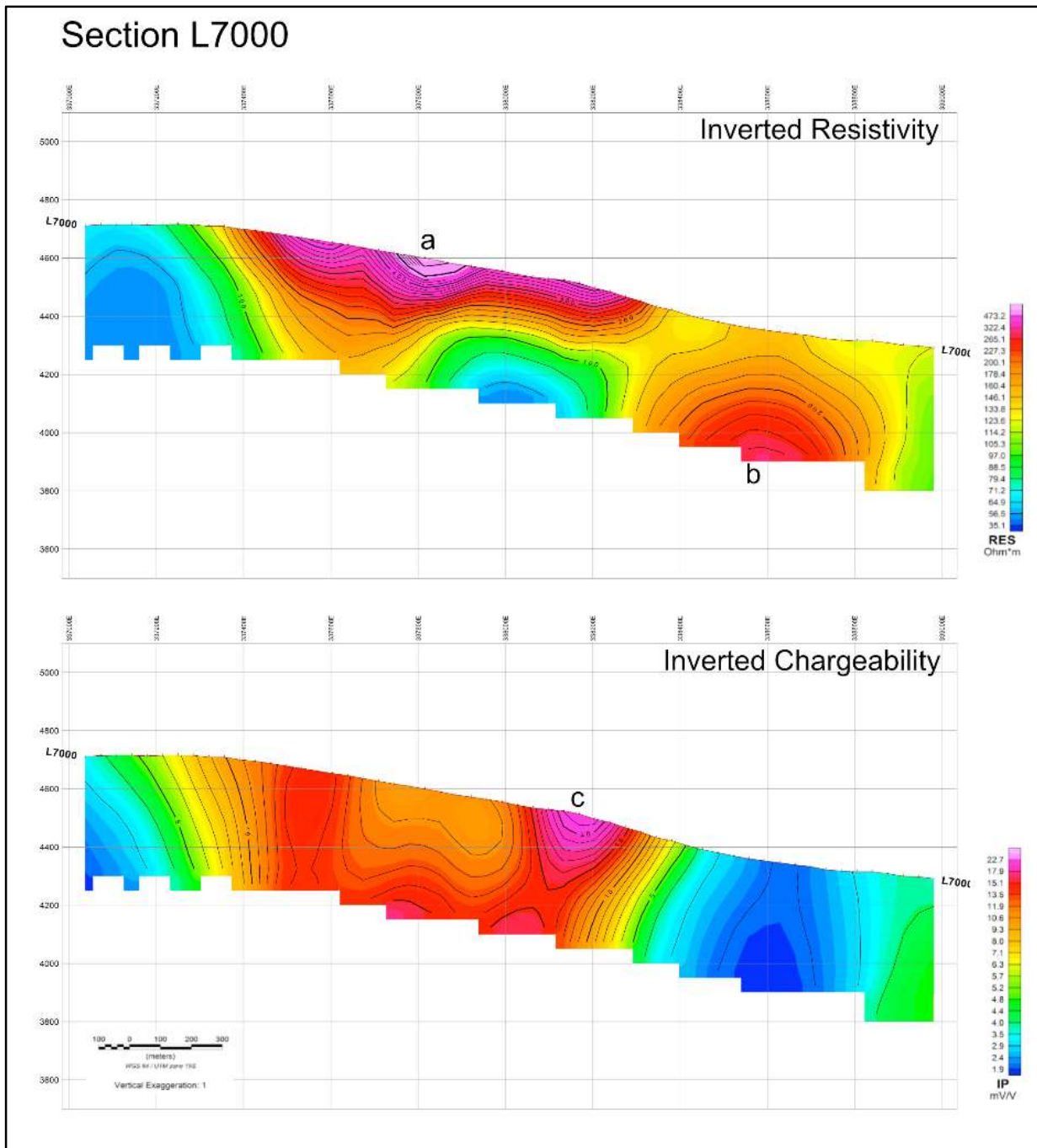
Following the geological work, it is recommended to run a program of diamond drilling with exploration targets greater than 300 m depth. Holes should be collared in the surface resistivity anomaly with the objective of evaluating the extension of surface geochemical anomalies.

Figure 16: Chargeability plotted at 150m below surface



3D inversion model. A linear, north-oriented band of high chargeability is prominent. Exposures along the road where it intersects the anomaly contain 5-10% fine grained disseminated pyrite in clay-altered volcanic units. A progressively deeper position of the pyrite-bearing zones is interpreted to cause the southern decline in chargeability along this band.

Figure 17: Inverted resistivity and chargeability sections from L7000.



Globetrotters 2021

(a) South-central resistivity anomaly with a sub-horizontal form near surface and the vertical root on the south end; (b) Northeast resistivity anomaly with moderate resistivity near surface and higher resistivity beginning at 4200 m elevation; (c) Expression of the central, north-trending chargeability anomaly.

The volcanic succession underlying the Property consists of andesite pyroclastic units interlayered with andesite lava, dacite pyroclastic units and dacite lava. The volcanic succession is sub-horizontal but individual units vary significantly laterally and vertically because of eruption processes. Accordingly, magnetic response is complicated by the primary distribution of the

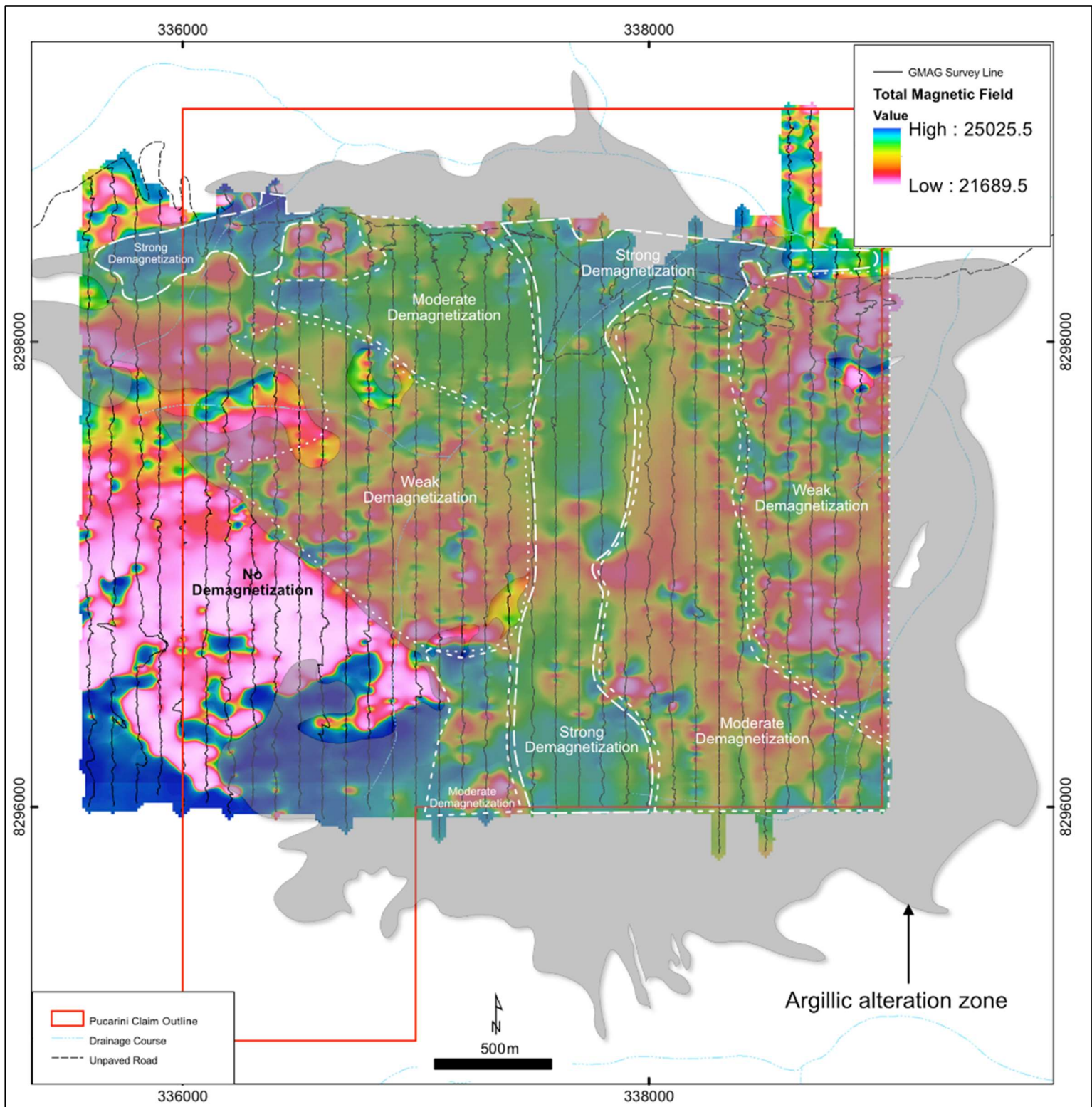
volcanic units and the effect of magnetite-destructive hydrothermal alteration. The broad zone of argillic alteration correlates well with domains of relatively low magnetic intensity; the most intense alteration corresponds with the lowest magnetic intensity. The geometry of magnetic patterns inside the alteration zones is consistent with mapped alteration zones. A north-trending domain of low magnetic intensity near the centre of the survey grid correlates with a distinctive high-chargeability zone.

The combined magnetic, resistivity, and chargeability data roughly define zonation of the three alteration types identified by field mapping. Although gold mineralization is not expected to directly correlate to geophysical anomalies, the prominent and continuous, north-trending vertical chargeability feature clearly visible in Figure 16 may be interpreted to be the main conduit for ascending hydrothermal solutions responsible for alteration and gold mineralization. It may have remained active for the lifetime of the hydrothermal system, beginning with the early, pyrite-dominant phase of hydrothermal alteration and continued through to the later stages of silica-dominant alteration, veining, and hydrothermal brecciation. The most pronounced surface expressions of this conduit are limited to elevations below 4,400 m where more intense alteration is spatially associated with highly anomalous gold values from outcrops. Alteration and veining restricted to narrow, vertical tabular zones with weak gold anomalies are separated by weakly altered host rock above this elevation. Zones of high resistivity partially overlap and flank the chargeability anomaly. The resistivity anomalies on the east side of the chargeability anomaly are blind beneath colluvium and weakly altered host rock.

Domains of reduced magnetic susceptibility correspond well with the extensive zone of argillic alteration outlined by outcrop mapping. Abundant primary magnetite in andesite and dacite volcanic units gives a low magnetic intensity response, which equates to high magnetic susceptibility in this region where the earth's magnetic field is horizontal. The type of hydrothermal alteration observed on the Property is magnetite-destructive and causes a reduction in magnetic susceptibility. Relatively weak alteration observed at surface in areas of low magnetic susceptibility suggest that hydrothermal alteration is more intense at depth.

Figure 18 illustrates the strong, moderate, and weak demagnetization domains overlain on argillic alteration interpreted from outcrop mapping, satellite imagery, spectral response, and spectral analysis of rock chips. Weak demagnetization is marked by decreased magnetic intensity and mottled texture. Moderate demagnetization is characterized by a decreased magnetic intensity and more uniform texture. Strong demagnetization has a low magnetic intensity and a quiescent texture. Increased separation between the magnetic sensor and demagnetized rock might explain the gradual increase in magnetic intensity southward along the north-trending strong demagnetization domain.

Figure 18: Map of total magnetic field outlining zones of strong, moderate, and weak demagnetization



Modified after Globetrotters 2021

## **10 DRILLING**

Forte Copper Corp. has not performed drilling on the Pucarini Property. To the best of the authors' understanding, the Property has never been tested by drilling.

## **11 SAMPLING PREPARATION, ANALYSES, AND SECURITY**

### **11.1 Rock Chip Sampling**

All outcrop sampling was conducted by the geological staff of Globetrotters Resources Peru SAC, who collected 214 rock samples from outcrops distributed across the Property, claim "GBT-92". Rock samples consisted of selective, channel, and panel samples. An industry-standard handheld GPS device was used to record sample locations by UTM coordinates in map datum WGS84, zone 19S. Lithology, alteration, mineralization, and other relevant information was recorded in a field notebook. Sample material was photographed and a witness (specimen) sample retained for reference from each sample. Field data recorded in the field was entered in an Excel spreadsheet which was imported into a relational database at the end of the field campaign.

The sample material was placed in marked, heavy-gauge plastic bags with a printed Company sample ticket fixed inside the bag. Individual samples were then placed into marked plastic-weave sacks and hand-delivered by Globetrotters staff to the ALS preparation laboratory in Arequipa.

At the ALS laboratory, samples are prepped for analysis by first being weighed individually, dried, then crushed with at least 70% of the sample passing through a 2 mm sieve. This material is split in two parts: one part is stored for future analyses and remainder is pulverized until 85% of sample is less than 75 µm in particle size.

Gold was analyzed by fire-assay of a 30 g sample pulp and finished with atomic absorption (AA) at a 0.005 ppm detection limit.

Multi-element analysis was completed on these samples using ALS's analytical package ME-ICP41 for thirty-five elements which uses aqua regia digestion and analysis by inductively coupled plasma-atomic emission spectrometry and mass spectrometry (ICP-MS). ME-ICP41 is considered a cost-effective approach to gathering geochemical information, but for the majority of natural rock matrices, assay data reported from an aqua regia chemical digestion should be considered as representing only the leachable portion of the rock sample.

Quality control of analysis of the rock chip samples was managed by ALS using their QA/QC protocols for geochemical assays.

### **11.2 Soil Sampling**

A total of 552 soil samples were collected over the IP geophysical grid by Globetrotters staff from October 28 to November 14, 2020. Sample locations were spaced at 50 m intervals along NE-



oriented IP survey lines. IP survey/soil sample lines were spaced 200 m apart. A handheld GPS device was used to locate samples sites.

Soil samples were collected from small, hand-dug holes ranging 5 to 30 cm in depth depending on the thickness of the organic soil horizon. Sampled material was collected from below the A soil horizon, if present, sieved with a 20-mesh sieve and sealed in plastic sample bags with a printed sample ticket. Sample identification number, location in UTM coordinates in map datum WGS84, Zone19S, and notes on soil sample characteristics including colour, humidity and fragment composition were recorded in a field notebook for each sample and this information was entered into an Excel spreadsheet. Information from the Excel spreadsheet was imported into a relational database at the end of the exploration program. Each sample bag was marked with a sample ID at the sample site, then placed in plastic weave bags and enclosed with a nylon security zip-tie. Samples were delivered by Globetrotters staff to the ALS preparation laboratory located in Arequipa.

Soils samples sent to ALS were dried and sieved to 80 mesh (-180  $\mu\text{m}$ ). Trace level analysis was carried out using multi-element method Super Trace AuME-ST43, an aqua regia digestion of a 25 g sample followed by an ICP-MS finish. Minimum detection limit for gold with this method is 0.001 ppm Au. Quality control of analysis of the soil samples was managed by ALS using their QA/QC protocols for geochemical assays.

### **11.3 Stream Sediment Sample**

A single stream sediment sample was collected from an active drainage in the vicinity of mineralized outcrop to determine if gold could be detected. Proper sampling equipment including a coarse sieve and sampling trowel were not available during sampling. The wet sample was transported to Arequipa to be dried and sieved with a 20-mesh sieve. The sample was submitted to the ALS laboratory for multi-element analysis by first screening to -180  $\mu\text{m}$ , and multi-element analysis using an aqua regia digestion and ICP-MS determination of element concentrations. Trace level analysis was carried out using multi-element method Super Trace AuME-ST43, an aqua regia digestion of a 25 g sample followed by an ICP-MS finish. Minimum detection limit for gold with this method is 0.001 ppm Au.

ALS employs a global quality management system that meets all requirements of International Standards ISO/IEC 17025:2017 and ISO 9001:2015. All ALS geochemical hub laboratories are accredited to ISO/IEC 17025:2017 for specific analytical procedures. The ALS quality program includes quality control steps through sample preparation and analysis, inter-laboratory test

### **11.4 Spectral Analysis**

Globetrotters staff collected 342 rock specimens for mineral identification by measuring and interpreting short wavelength infrared spectra. Rock specimens approximately 3 x 3 cm in size were chipped from outcrops and placed in small plastic ziplock bags with a sample identification number corresponding to a GPS location recorded in UTM coordinates in map datum WGS84, zone 19S. Notes describing lithology and alteration were recorded in a field notebook and entered into an Excel spreadsheet. Samples were submitted to ALS in Arequipa for spectra measurement and interpretation by ALS staff in Lima. ALS uses a TerraSpec instrument for measuring the short

wavelength infrared spectra of submitted samples (ALS Code: HYP-PKG). Interpretation is done using aiSIRIS analysis software. Mineralogy and spectral features are provided via digital file.

## **12 DATA VERIFICATION**

On November 22, 2020, one of the authors (Park) visited the Pucarini property and examined several locations and collected six rock sample (Figure 19 and Figure 20). See Figure 9 for confirmation sample locations.

Mr. Park is of the opinion that the historical data descriptions of sampling methods and details of location, number, type, nature, and spacing or density of samples collected, and the size of the area covered are all adequate for the current stage of exploration for the Property.

Six verification rock chip samples were collected on the Pucarini property during the field visit. Five samples came from previously sampled outcrops that yielded anomalous gold values that were not intended to be close replicate samples. One sample is from an outcrop that had not previously been sampled. All samples were taken as panel rock chips either oriented horizontally or vertically as noted in the sample description in Table 3. Most samples were taken from outcrops containing multiple, narrow, sub-parallel silicified structures or broad silicified ribs forming linear outcrops. One brecciated quartz vein measuring 20 cm in width was sampled excluding wall rock.

Mr. Park's rock samples were sent to ALS Peru S.A. in Lima and underwent analysis for 35 element Aqua Regia ICP AES (ME-ICP41) and Au 30 g Fire Assay with an ICP-AA finish (Au-AA23). ALS Peru is ISO/IEC 17025:2005. Forte Copper Corp., Globetrotters, and the authors are independent of ALS Peru (see Table 4 for select assays).

Mr. Park collected approximately 2 kg of material for each sample. Samples bags were ticketed and closed in the field (Figure 22), then transported with the author to Juliaca on Sunday night, November 22, 2020. The following morning the samples were loaded into two sealed rice sacks and shipped by commercial transport to the ALS prep lab in Arequipa. These samples were in the author's possession at all times except for passing the night in the locked field vehicle parked in an enclosed and secured parking area controlled by the hotel where our crew spent the night.

Mr. Park observed evidence of the recent geophysical survey completed on the property. The Induced Polarization lines were oriented NE-SW with grid lines spaced 200 m apart and survey points at 50m spacing along lines (Figure 23). Each survey point was marked initially with a small rock monument and red flagging. Flagging was removed after the points were surveyed. Ground mag survey lines ran N-S and spaced 100 m apart without markers.

Mr. Park observed evidence of the soil sampling program where samples had been collected at each IP grid marker. Samples were collected from a small hole that passed through the organic A soil horizon, if present. Sample site holes were refilled after sampling (Figure 21).

The author Strickland has not undertaken a personal inspection of the Pucarini Property. Mr. Strickland did randomly check 50 of the assay results in the ArcView database provided against the assays certificates provided and did not detect any irregularities between the two.

Figure 19: Outcrop sampling in the altered zone.



Note that outcrops are rare. Geophysical grid marker on outcrop to the left of samplers

Figure 20: Steve Park on the north ridge



Figure 22: Closed sample bag with sample ticket secured in place



Figure 21: Close-up of soil sample site, Line 7200



Figure 23: Rock marker with red flagging indicating a point on geophysical line.



Table 3: Author Sample Collection Notes

Check Sample ID	WGS84		Panel Samples		Structure			Lith	Breccia	Alteration						Description
	East	North	Size (m)	Dir	Wd (m)	Strike	Dip			Silcf	Py	Lim	Gt	Hem	Aln	
30020	337529	8296227	1.0x2.0	vert	0.5	350	75E	Andesite	N/A	3	0	2	1	0	0	Minor casts of cubic pyrite <1mm
30021	338323	8297582	1.0x1.0	hrz	N/A	N/A	NA	Andesite	N/A	2	1	3	3	0	0	Minor vuggy silica
30022	337475	8297138	0.2x1.5	hrz	0.2	270	90	Andesite	Hydrothermal	3	2	2	2	0	2	Crystalline alunite in vugs. Wall rock massive silcf, feldspar phns to clay
30023	337069	8298091	0.6x1.0	hrz	0.6	270	75N	Andesite	Hydrothermal	3	1	2	3	0	0	Fine drusy quartz, boxwork gt, vf py dssm in silcf mtx
30024	337119	8298039	0.5x1.0	vert	0.5	350	90	Andesite	Hydrothermal	3	1	2	3	0	0	Vf white veinlets of supergene
30025	337366	8297762	2.0x2.0	vert	2.0	70	90	Andesite	Hydrothermal	2	0	0	2	0	0	Auto-clasts in rock flour mtx, silcf

Silcf = silicification/silicification  
 Py = pyrite  
 Lim = limonite  
 Gt = goethite  
 Hem = hematite  
 dssm = disseminated  
 mtx = matrix  
 phns = phenocrysts  
 vf = very fine  
 3 = Strong  
 2 = Moderate  
 1 = Minor  
 0 = Not observed

Table 4: Select Author Check Assays

Check Sample ID	Original Sample ID	Company Assays			Author Assays		
		Au ppm	Ag ppm	As ppm	Au ppm	Ag ppm	As ppm
30020	3377	<0.005	<0.2	17	<0.005	<0.2	10
30021	3769	0.484	<0.2	19	0.500	0.4	14
30022	3762	6.890	2.6	204	2.300	0.4	48
30023	3601	0.872	0.5	129	0.544	0.3	115
30024	N/A				0.469	0.6	181
30025	3499	0.005	<0.2	23	0.012	<0.2	29

The results of this limited check sampling exercise serve to confirm the anomalous values of gold reported by the Company from Globetrotter's rock chip sampling program and suggest that there were no systematic biases in the sampling program. Both field and laboratory methods appear to have been adequate to obtain verifiable and generally reproducible results.

Given the results of the check-sampling and a review of all geochemical data presented, the authors believe that industry best-practice standards were used by Globetrotters in conducting the surface geochemical sampling program on the Property and are of the opinion that the data verification program completed on the data collected from the Property appropriately support the database quality and the geologic interpretations derived therefrom.

### **13 MINERAL PROCESSING AND METALLURGICAL TESTING**

Forte Copper Corp. has not undertaken metallurgical test work on material from the property.

### **14 MINERAL RESOURCE ESTIMATE**

There is no current mineral resource on the Pucarini Property.

### **15 THROUGH 22 ARE NOT APPLICABLE TO THIS REPORT**

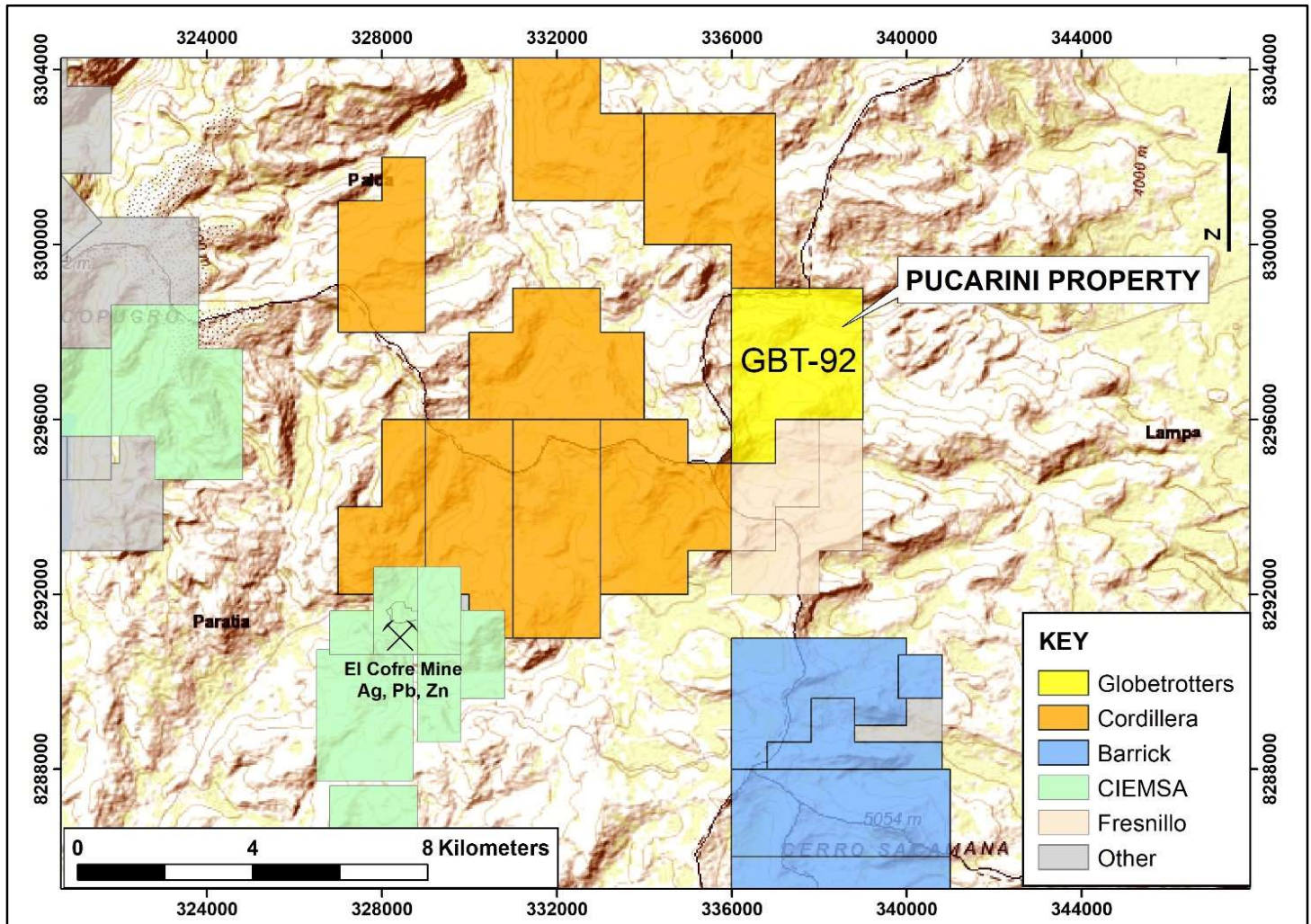
Items 15 through 22 of Form 43-101F1 do not apply to the Property that is the subject of this technical report as this is not an advanced property.

### **23 ADJACENT PROPERTIES**

The Pucarini Property shares its southern boundary with mining concessions held by Fresnillo Peru SAC covering an area of 1,000 has. A concession block of 2,000 has. held by Cordillera Resources is contiguous with the Property to the north. Cordillera Resources hold another large block of 4,500 has. immediately west and southwest of the Property (Figure 24).

No known mineral occurrences are within 5 km of the property. Anecdotal evidence of a small mine working close to the southern boundary of the Property has not been confirmed by the Company. The nearest mining operation is the El Cofre Mine (Ag-Pb-Zn) located 10 km southwest of the Property.

Figure 24. Map of mining concessions adjacent to and near the Property



## 24 OTHER RELEVANT DATA AND INFORMATION

The authors are not aware of any other relevant information at this time.

## 25 INTERPRETATION AND CONCLUSIONS

The Company carried out an exploration program on the Pucarini Project of consisting of geochemical and geophysical surveys and geologic mapping with the objective of defining exploration targets that warrant testing by drilling.

Alteration style and mineralogy exposed on the Property is consistent with high-sulphidation gold systems described in Peru, throughout the Andes, and globally. This deposit model is the theory being tested in the work done to date and planned for in future programs. Alteration mapping completed over the property outlines a hydrothermal system with minimum surface expression of 3 x 4 km, which encompasses gold mineralization in several linear zones with strike lengths ranging from 500 to 2,500 m. Hydrothermal alteration crudely corresponds with magnetic, resistivity, and chargeability responses. Outcrop sampling demonstrates gold is a component of the hydrothermal system but correlating gold mineralization with geophysical response is not possible with the current level of geological information and understanding.

The prominent chargeability anomaly bisecting the IP grid coinciding with a domain of low magnetic intensity is interpreted as a vertical pyrite-bearing clay alteration zone formed early in the evolution of the hydrothermal system. This north-trending zone is considered the primary conduit for rising hydrothermal solutions. Zones of relatively high resistivity partially overlap and flank the chargeability anomaly. Silica introduced after clay-pyrite alteration is one possible explanation for the high-resistivity zones. The size of the high-resistivity anomalies suggests silica alteration is more extensive in the subsurface.

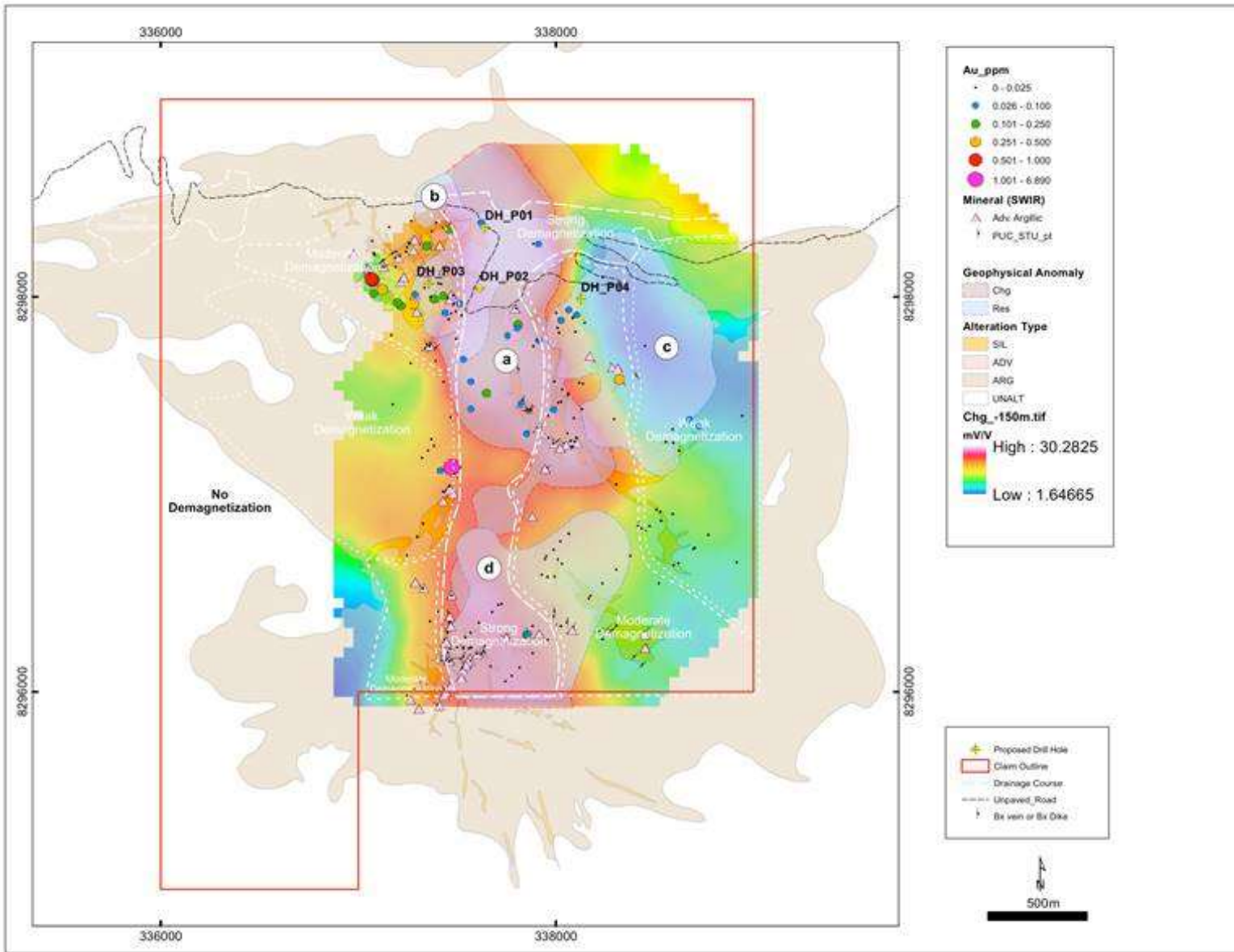
There is no evidence of extensive vuggy silica, water-table controlled lithocap, or granular silica as described at other deposits. The observed alteration mineral assemblages containing diaspore, alunite, and pyrophyllite are indicative of higher alteration fluid temperature and suggest the erosion level coincides with the base of the shallowest part of the epithermal thermal system. Available outcrop samples show gold is confined to 0.1 to 5.0 metre wide, sub-vertical breccia dikes and breccia veins with orientations that mimic the property-scale structural trends. Geophysical evidence indicates these structures coalesce at depth into more continuous and wider mineralized zones. Permeable layers in the volcanic sequence could promote development of horizontal mineralization zones.

Summary of key target areas and proposed drill holes (Figure 25):

- A. A linear, north-trending chargeability anomaly which coincides with a domain of strong demagnetization.
- B. Resistivity high anomaly that overlaps and extends west from the chargeability anomaly. A cluster of anomalous gold in outcrop and multiple breccia veins containing advance argillic mineralogy occur immediately west of the resistivity anomaly.
- C. Resistivity high anomaly located immediately east of the chargeability anomaly.

D. Coincident chargeability, resistivity and demagnetization associated with an array of breccia veins and breccia dikes containing advanced argillic mineralogy. Chargeability and resistivity anomalies are from modeled response at -150 metres below surface. Quartz veins, breccia veins, and breccia dikes strike northwest, north and northeast.

Figure 25: Map showing a summary of key exploration targeting evidence and proposed drill hole locations



After Globetrotters 2021



## 26 RECOMMENDATIONS

In the authors' opinion, Pucarini is a property of merit that justifies the continuation of exploration programs designed to test the deposit model outlined in this report.

The exploration targets established by geological mapping, geochemical sampling, and geophysical surveys require drilling as the next step in testing for gold mineralization. An initial phase of drilling is recommended to test four (4) targets with 1,000 metres of core drilling. Core drilling is recommended to obtain the geological information required to adequately determine controls on gold mineralization and increase confidence in subsequent exploration decisions.

Drill holes will be positioned to test these geophysical anomalies where coincident with elevated gold values. Locations of these drill holes may be modified following further interpretation of the exploration program's database by the Company's geologic staff.

The first hole, DH\_P01, is designed to test the north end of the north-trending chargeability anomaly where it coincides with a resistivity anomaly and a domain of strong demagnetization. This hole will be collared near outcrops of hydrothermal breccia containing ~5% fine-grained disseminated pyrite.

Drill hole DH\_P02 is positioned to test a northwest-trending zone defined by abundant quartz veining, hydrothermal breccia veins and breccia dikes associated with an advanced argillic mineral assemblage. This hole will be located where the vein zone intersects the north-trending chargeability anomaly and coincident resistivity anomaly.

Drill hole DH\_P03 is designed to test beneath the cluster of rock chip samples that returned anomalous gold values that coincide with advanced argillic alteration and a resistivity anomaly on the west flank of the north-trending chargeability anomaly.

Drill hole DH\_P04 is positioned to test the large resistivity anomaly on the east flank of the north-trending chargeability anomaly where it intersects the northern margin of the northwest-trending zone of veining.

Table 5 outlines the estimated cost in Canadian dollars to drill test the highest priority targets established from geological, geochemical and geophysical evidence.

Table 5: Proposed Budget for DDH Drill Program

Item	Quantity	Units	Unit Cost (CAD\$)	Total (CAD\$)
Community Relations	1	year	60,799	60,799
Drill permitting	1	contract	94,760	94,760
Field Support	1	month	22,110	22,110
Site Preparation/Rehabilitation	6	days	2,596	15,576
Drilling	1000	metres	368	368,000
Analysis	735	samples	60	44,100

Accommodation/Travel	1	month	19,760	19,760
Salary	1	month	32,011	32,011
Sub-total				657,116
Contingency	5	percent		32,856
<b>Total</b>				<b>689,972</b>

## 27 REFERENCES

- Allis, R.G., 1990, Geophysical anomalies over epithermal systems: in Hedenquist, J.W., White, N.C., and Siddeley, G., eds., *Epithermal Gold Mineralization of the Circum-Pacific; Geology, Geochemistry, Origin and Exploration*, II. Volume 36 (1/3): *Journal of Geochemical Exploration*, Elsevier, p. 339–374.
- Anderson, J.A., 1982, Characteristics of leached capping and techniques of appraisal; in: TITLEY, S.R García W., *Geología de los cuadrángulos de Puquina (34-t), Omate (34-u), Huaitire (34-v), Mazo Cruz (34-x) y Pizacoma (34-y)*, INGEMMET, bol. 29-a
- Arribas, A., Jr., Hedenquist, J. W., Itaya, T., Okada, T., Concepcion, R. A., and Garcia, J. S., Jr., 1995. Contemporaneous formation of adjacent porphyry and epithermal Cu-Au deposits over 300 ka in northern Luzon, Philippines, *Geology*, v. 23, p. 337–340.
- Arribas, Antonio, Jr., 1995, Characteristics of high-sulphidation epithermal deposits, and their relation to magmatic fluid: *Mineralogical Association of Canada Short Course*, v. 23, p. 419–454.
- Atherton, M., Pitcher, W. and Warden, V., 1983. The Mesozoic Marginal Basin of Central Peru, *Nature*, v. 305, p. 303-305.
- Atherton, M., Warden, V., and Sanderson, L. M., 1985. The Mesozoic marginal basin of central Peru: a geochemical study of within plate-edge volcanism, in Pitcher, W.S. et al., eds., *Magmatism at a plate edge: The Peruvian Andes*: Glasgow, Blackie, John Wiley and Sons, p. 47-58.
- Atkin B., Espinoza. I., and Peter, H. 1981, Cu-Fe mineralization in Arequipa. Department of Geology of Nottingham, Nottingham I ZG7 2RD, United Kingdom.
- Audebaud, EG. Laubacher, and R. Marocco, 1976, Coupe géologique des Andes de Perou de l'Océan Pacifique au Bouclier brésilien: *Geol. Rundschau*, v. 65, p. 223-264.
- Barriero, B.A. and Clark A.H., 1984. Lead Isotopic evidence for Evolutionary Changes in MagmaCrust Interaction, Central Andes, southern Peru, *Earth and Planetary Science Letters*, v.69, p. 30-42
- Barton, P.B., and Skinner, B.J., 1967, Sulfide mineral stabilities: in Barnes, H.L., ed., *Geochemistry of Hydrothermal Ore Deposits*: Holt, Rinehart and Winston, New York, p. 236–333.
- Bell, P.D., Gomez, J.G., Loayza, C.E., and Pinto, R.M., 2004. Geology of the gold deposits of the Yanacocha district, northern Peru: PACRIM 2004 Conference, Adalaide, Proceedings of the Pacrim 2004 Conference, Australasian Institute of Mining and Metallurgy (AusIMM), Carlton, p. 19–22.
- Bellido, E., 1979. *Geología del cuadrángulo de Moquegua (hoja: 35-u)*: Lima, Peru, Instituto Geológico Minero y Metalúrgico, 78 p.
- Benavides, V., 1956. Cretaceous System in Northern Peru, *Bulletin of the American Museum of Natural History*, v. 108, p. 252-494.
- Benavides-Cáceres, V., 1999, Orogenic Evolution of the Peruvian Andes: The Andean Cycle: in Skinner, B.J., ed., *Geology and Ore Deposits of the Central Andes: Society of Economic Geology Special Publications*, no. 7, Society of Economic Geologists, Littleton, USA, p. 61–107.

Bethke, P.M., 1984. Controls on base and precious metal mineralization in deeper epithermal environments: Open File Report 84-890, US Department of the Interior, Geological Survey, Reston, VA, USA, 38 p.

Clark, A. H., Tosdal, R. M., Farrar, E. and Plazolles V. A., 1990. Geomorphic environment and age of supergene enrichment of the Cuajone, Quellaveco, and Toquepala porphyry Cu deposits, southeastern Peru, *Economic Geology*, v. 85, p. 1604-1628.

Clark, A.H., Farrar, E., Kontak, D.J., Langridge, R.J., Arenas F., M.J., France, L.J., McBride, S.L., Woodman, P.L., Wasteneys, H.A., Sandeman, H.A., and Archibald, D.A., 1990, Geologic and geochronologic constraints on the metallogenic evolution of the Andes of southeastern Peru: *Economic Geology*, v. 85, p. 1520–1583.

Coira, B., Davidson, J., Mpodozis, C. and Ramos, V., 1982. Tectonic and Magmatic Evolution of the Andes of northern Argentina and Chile, *Earth Science Reviews*, v. 18, p. 302-332.

Cooke, D.R., Hollings, P., and Chang, Z., 2011, Philippine porphyry and epithermal deposits: an introduction: *Economic Geology*, v. 106, p. 1253–1256.

Corbett, G. 2013. Pacific Rim Epithermal Au-Ag - Keynote Address. World Gold Conference (pp. 5-13). Brisbane: Australasian Institute of Mining and Metallurgy.

Dalmayrac, B., Laubacher, G. Marocco, R. (1980) Géologie des Andes Péruviennes. Caractères généraux de l'évolution géologique des Andes péruviennes Travaux et Document de l'ORSTROM. v. 122, 501 pp.

Davidson, J. and Mpodozis, C., 1990. Regional geologic setting of epithermal gold deposits, Chile, *Economic Geology*, v. 86, p. 1174-1186.

Douglas, J.A (1920) *Quarterly Journal of the Geological Society*, 76, 1-61, 1 October 1920, <https://doi.org/10.1144/GSL.JGS.1920.076.01-04.02>

Einaudi, M.T., Hedenquist, J.W., and Inan, E.E., 2003, Sulphidation state of fluids in active and extinct hydrothermal systems: Transitions from porphyry to epithermal environments: in Simmons, S.F., and Graham, I., eds., *Society of Economic Geologists Special Publication 10: Volcanic, Geothermal, and Ore-Forming Fluids: Rulers and Witnesses of Processes Within the Earth: Society of Economic Geologists Special Publication 10*, Society of Economic Geologists, Inc., Littleton, CO, p. 285–313.

Field, C. W., Michael, B, and Bruce, W., 1974, Porphyry Copper - Molybdenum Deposits of the pacified Northwest. *Transactions - Vol 255*, Society of Mining Engineers, ALME, man-hp 9-22.

Giggenbach, W.F., 1988, Geothermal solute equilibria. Derivation of Na-K-Mg-Ca geothermometers: *Geochimica et Cosmochimica Acta*, v. 52, p. 2749–2765.

Giggenbach, W.F., 1997, The origin and evolution of fluids in magmatic-hydrothermal systems.: in Barnes, H.L., ed., *Geochemistry of hydrothermal ore deposits*. 3rd Edition: John Wiley and Sons, New York, p. 737–796.

Gustafson, L. B., and Hunt, J. P., 1975. The porphyry copper deposit at El Salvador, Chile: *Economic Geology*, v. 70, p. 857–912.

H.L. Barnes, ed., 1979. Sulfide mineral stabilities, *Geochemistry of Hydrothermal Ore Deposits*, John Wiley and Sons, New York, 404 p.

Harvey, B.A., Myers, S.A., Klein, T., and Weber, G., 1999. Yanacocha gold district, northern Peru: Pacrim '99 Congress, Proceedings of the Pacrim'99 Congress, Australasian Institute of Mining and Metallurgy, Bali, p. 445–459.

Hedenquist, Jeffrey & Izawa, Eiji & Arribas, Antonio & White, N.C. (1996). Epithermal gold deposits: Styles, characteristics, and exploration: Poster and booklet, *Resource Geology Special Publication 1*, 17 p.

Hedenquist, J.W., 1987. Mineralization associated with volcanic-related hydrothermal systems in the circum-Pacific Basin: Transactions of the Geology Special Fourth Circum-Pacific Energy and Mineral Resources Conference, American Association of Petroleum Geology, Singapore, p. 513–524.

Hedenquist, J.W., 1995, The ascent of magmatic fluid: Discharge versus mineralization: Mineralogical Association of Canada Short Course, v. 23, p. 263–289.

Hedenquist, J.W., and Lowenstern, J.B., 1994, The role of magmas in the formation of hydrothermal ore deposits: *Nature*, v. 370, p. 519–527.

Hedenquist, J.W., Arribas, A., and Gonzalez-Urien, E., 2000, Exploration for epithermal gold deposits: *Reviews in Economic Geology*, v. 13, p. 45–77.

Hedenquist, J.W., Arribas, A., and Reynolds, T.J., 1998, Evolution of an intrusion-centered hydrothermal system; Far Southeast-Lepanto porphyry and epithermal Cu-Au deposits, Philippines: *Economic Geology*, v. 93, p. 373–404.

Hedenquist, J.W., Matsuhisa, Y., Izawa, E., White, N.C., Giggenbach, W.F., and Aoki, M., 1994, Geology, geochemistry, and origin of high sulphidation Cu-Au mineralization in the Nansatsu District, Japan: *Economic Geology*, v. 89, p. 1–30.

Henley, R.W., 1985, The geothermal framework for epithermal deposits: in Berger, B.R., and Bethke, P.M., eds., *Geology and Geochemistry of Epithermal Systems: Reviews in Economic Geology*, v. 2, Society of Economic Geologists, Littleton, USA, p. 1–24.

Hudson, D.M., 2003, Epithermal alteration and mineralization in the Comstock district, Nevada: *Economic Geology*, v. 98, p. 367–385.

Irvine, R.J., and Smith, M.J., 1990, Geophysical exploration for epithermal gold deposits: in Hedenquist, J.W., White, N.C., and Siddeley, G., eds., *Epithermal Gold Mineralization of the Circum-Pacific; Geology, Geochemistry, Origin and Exploration*, II. Volume 36 (1/3): *Journal of Geochemical Exploration*, Elsevier, p. 375–412.

Isacks B. L., 1988. Uplift of the central Andean plateau and bending of the Bolivian orocline, *Journal of Geophysical Research*, v. 93, p. 3211-3231.

Jaillard, E., Hérail, G., Monfret, T., Díaz-Martínez, E., Baby, P., Lavenu, A., and Dumont, J.F., 2000. Tectonic evolution of the Andes of Ecuador, Peru, Bolivia and northernmost Chile, In Cordani, U.G., Milani, E.J., Thomaz Filho, A., and Campos, D.A., eds., *Tectonic Evolution of South America; 31st International Geological Congress, Rio de Janeiro, Brazil, August 6–17, 2000, Proceedings*, p. 481–559.

Jannas, R.R., Beane, R.E., Ahler, B.A., and Brosnahan, D.R., 1990, Gold and copper mineralization at the El Indio deposit, Chile: in Hedenquist, J.W., White, N.C., and Siddeley, G., eds., *Epithermal Gold Mineralization of the Circum-Pacific; Geology, Geochemistry, Origin and Exploration*, II, 36(1-3): *Journal of Geochemical Exploration*, Elsevier, p. 233–266.

Jenks, W.F., 1946, Preliminary note on geologic studies of the Pacific Slope in southern Peru: *American Journal of Science*, v. 244, p. 367–372.

Klinck, B. A., Ellison, R.H., Hawk, M.P. 1986. The geology of the Cordillera occidental and Altiplano, West of the Lake Titicaca, Southern Peru. Instituto de Geología, Minería y Metalurgia. Lima, preliminary Report.

Laubacher, G. 1978. Géologie de la Cordillère orientale et de l'Altiplano au Nord et Nord-Ouest du Lac Titicaca (Pérou). *Travaux et Documents de l'ORSTOM* 95, Paris

Les Oldham, D., Davila Juan, R., Placido, D. Gonzales, R. (2018) Geological Explorations Annual Report Chapi project By: Anglo Peruana SA Terra for Nexa Resources Peru SAA. Company Internal Document

Lindgren, W., 1933. *Mineral deposits: 4th Edition*, McGraw-Hill, New York, 930 p.

McKee, E.H., and Noble, D.C., 1989, Cenozoic tectonic events, magmatic pulses, and base and precious-metal mineralization in the Central Andes: in Ericksen, G.E., Canas Pinochet, M.T., and Reinemund, J.A., eds., *Geology of the Andes and Its Relation to Hydrocarbon and Mineral Resources*, vol. 11: *Circum-Pacific Council for Energy and Mineral Resources Earth Sciences Series*, Houston, p. 189–194.

Megrad 1987. Cordilleran and marginal Andes: a review of Andean geology North of the Arica elbow (18%). In: MONGER, J. W. H. & FRANCHETEAU, J. (eds) *Circum-Pacific belts and evolution of the Pacific Ocean basin*. American Geophysical Union, *Geodynamic series*, 18, 71-95

Mpodozis, C. and Ramos, V., 1989. The Andes of Chile and Argentina, In Erickson, G.E., Cañas Pinochet, M.T. and Reynemund, J.A., eds., *Geology of the Andes and its relations to hydrocarbon and mineral resources*, *Circum-Pacific council for Energy and Mineral Resources Earth Science Series*, v. 11, p. 59-90.

Mukasa, S. B., 1986. Common Pb isotopic compositions of the Lima, Arequipa, and Topqepala segments of the coastal batholith, Peru implications for magma genesis, *Geochimica et Cosmochimica Acta*, v. 50, p. 771–782

Newell, N. D. 1949. *Geology of the Lake Titicaca region, Peru and Bolivia*. *Memoir of the Geological Society of America*, 36, 111 pp.

Noble, D. C., McKee, E. H., Eyzaguirre, V. R., and Marocco, R., 1984. Age and regional tectonic and metallogenic implications of igneous activity and mineralization in the Andahuaylas-Yauri belt of Southern Peru, *Economic Geology*, v. 79, p. 172-176.

Palacios Moncayo, O., De la Cruz Wetzell, J.S., De la Cruz Bustamante, N.S., Klinck, B.A., Ellison, R.A., and Hawkins, M.P., 1993, *Geología de la Cordillera Occidental y Altiplano al Oeste del Lago Titicaca Sur del Perú (Proyecto Integrado del Sur)*. Hojas: 31-t, 31-u, 31-v, 31-x, 31-y, 32-s, 32-t, 32-u, 32-v, 32-x, 32-y, 33-v, 33-x, 33-y, 33-z- [Boletín A 42]:

Panteleev, A., 1995. Porphyry Cu-Mo-Au. En D. a. Lefebure, Selected British Columbia Mineral Deposit Profiles (págs. 87-92). British Columbia Ministry of Mines.

Pitcher, W. S., 1983. Granite type and tectonic environment, *in* Hsu, K. J., ed., Mountain building processes: London, Academic Press, p. 19-40.

Pitcher, W.S., 1985, A multiple and composite batholith: in Pitcher, W.S., Atherton, M.P., Cobbing, E.G., and Beckinsale, R.D., eds., Magmatism at a plate edge: The Peruvian Andes: Blackie, Glasgow, p. 93–101.

Quang, C.S., Clark, A.H., Lee, J.K.W. and Guillen, B.J., 2003 - <sup>40</sup>Ar-<sup>39</sup>Ar Ages of Hypogene and Supergene Mineralization in the Cerro Verde-Santa Rosa Porphyry Cu-Mo Cluster, Arequipa, Peru: in *Econ. Geol.* v.98, pp. 1683-1696.

Quang, C.S., Clark, A.H., Lee, J.K.W. and Hawkes, N., 2005 - Response of Supergene Processes to Episodic Cenozoic Uplift, Pediment Erosion, and Ignimbrite Eruption in the Porphyry Copper Province of Southern Peru: in *Econ. Geol.* v.100, pp. 87-114.

Rainbow, A., Clark, A.H., Kyser, T.K., Gaboury, F., and Hodgson, C.J., 2005, The Pierina epithermal Au–Ag deposit, Ancash, Peru: paragenetic relationships, alunite textures, and stable-isotope geochemistry: *Chemical Geology*, v. 215, p. 235–252.

Ramos, V. A., 2009. Anatomy and global context of the Andes: Main geologic features and the Andean orogenic cycle: *Geological Society of America Memoir*, v. 204, p. 31–65.

Ramos, V.A., 1988. The tectonics of the Central Andes: 30° to 33°S latitude (1988) Processes in Continental Lithospheric Deformation, pp. 31-54., Clark, S, and Burchfiel, D, eds, *Geological Society of America Special Paper* 218, p

Sandeman, H.A., Clark, A.H., and Farrar, E., 1995, An integrated tectono-magmatic model for the evolution of the southern Peruvian Andes (13-20 S) since 55 Ma: *International Geology Review*, v. 37, p. 1039–1073.

Sawkins, F.J., 1990. Metal deposits in relation to plate tectonics. Second Edition: *Minerals, Rocks and Mountains*, 17, Springer-Verlag, Berlin, 461 p.

Schalamuk, I.B., Zubia, M., Genini, A., and Fernandez, R.R., 1997, Jurassic epithermal Au–Ag deposits of Patagonia, Argentina: *Ore Geology Reviews*, v. 12, p. 173–186.

Sébrier. M., Lavenu A., Fornari, M., and Soulas, J.P., 1988. Tectonics and uplift in central Andes (Peru, Bahia and northern Chilc) from Eocene to Present. *Géodynamique*, 3: 85-106

Sillitoe, R. H., 1976. Metallic mineralization affiliated to sub-aerial volcanism: a review. *Proceedings Annual Meeting of the Geological Society, London-Institution of Mining and Metallurgy*, p. 99-116.

Sillitoe, R. H., 1977. Permo-Carboniferous, Upper Cretaceous and Miocene porphyry copper type mineralization in the Argentinean Andes, *Economic Geology*, v. 72, p. 99-103.

Sillitoe, R. H., 1988. Epochs of intrusions related Cu mineralization in the Andes, *Journal of South American Earth Sciences*, v. 1, p. 89-108.

Sillitoe, R.H., 1993, Epithermal models—genetic types, geometric controls and shallow features: Geological Association of Canada Special Paper 40, p. 403–417.

Sillitoe, R. H., 1997. Characteristics and controls of the largest porphyry copper-gold and epithermal gold deposits in the circum-Pacific region, Australian Journal of Earth Sciences, v. 44, p. 373-388.

Sillitoe, R. H., 2010. Porphyry copper systems: Economic geology, v. 105, p. 3–41.

Sillitoe, R. H., and Perelló, J., 2005. Andean copper province: Tectonomagmatic settings, deposit types, metallogeny, exploration, and Discovery, Economic Geology, 100th anniversary volume, p. 845–890.

Sillitoe, R.H., 2010, Porphyry copper systems: Economic Geology, v. 105, p. 3–41.

Sillitoe, R.H., and Hedenquist, J.W., 2003, Chapert 16: Linkages between volcanotectonic settings, ore-fluid compositions, and epithermal precious metal deposits: eds., Society of Economic Geologists Special Publication 10: p. 315–343.

Simmons, A., 2013. Magmatic and Hydrothermal Stratigraphy of Paleocene and Eocene Porphyry Cu-Mo Deposits in Southern Peru, Ph.D. Thesis University of British Columbia

Simmons, S.F., White, N.C., and John, D.A., 2005, Geological characteristics of epithermal precious and base metal deposits: in Hedenquist, J.W., Thompson, J.F.H., Goldfarb, R.J., and Richards, J.P., eds., Economic Geology 100th Anniversary Volume, 1905-2005: Econ Geol, Society of Economic Geologists, Inc., Littleton, CO, p. 485–522.

Stewart, J.W., Evernden, J.F., and Snelling, N.J., 1974, Age determinations from Andean Peru: a reconnaissance survey: Geological Society of America Bulletin, v. 85, p. 1107–1116.

Stoffregen, R.E., 1987, Genesis of acid-sulfate alteration and Au-Cu-Ag mineralization at Summitville, Colorado: Economic Geology, v. 82, p. 1575–1591.

Streckeisen, A. L., 1974. Classification and nomenclature of plutonic rocks. Recommendations of the IUGS subcommission on the systematics of igneous rocks: Geologische Rundschau, v. 63, p. 773–785.

Teal, L., and Benavides, A., 2010, History and geologic overview of the Yanacocha mining district, Cajamarca, Peru: Economic Geology, v. 105, p. 1173–1190.

Tosdal, R. M., Clark, A. H., and Farrar, E., 1981. K-Ar geochronology of the late Cenozoic volcanic rocks of the Cordillera Occidental, southernmost Peru, Journal of Volcanology and Geothermal Research, v. 10, p. 157-173.

Tosdal, R. M., Clark, A. H., and Farrar, E., 1984. Cenozoic polyphase landscape and tectonic evolution of the Cordillera Occidental, southernmost Peru, Geological Society of America Bulletin, v. 95, p. 1318-1332.

Tosdal, R. M., and Richards, J.P., 2001. Magmatic and structural controls on the development of Porphyry Cu ±Mo ±Au deposits, Reviews in Economic Geology, v. 14, p. 157-181.

Tumialan, P.H., (Ed.) 2003 - Cerro Verde, Santa Rosa y Cerro Negro: in Tumialan, P.H., (Ed.) 2003 Compendio de Yacimientos Minerales del Peru, Instituto Geologico Minero y Metalurgico, Republic del Peru, Capitulo VII, Porfidos de Cobre, Boletin no. B-10, pp. 137-139, 141 (in Spanish with English translation).



Valencia, V. A., Ruiz, J., Barra, F., Gehrels, G., Ducea, M., Titley, S. R., and Ochoa-Landin, L., 2005. U-Pb zircon and Re-Os molybdenite geochronology from La Caridad porphyry copper deposit: Insights for the duration of magmatism and mineralization in the Nacozari District, Sonora, Mexico, *Mineralium Deposita*, v. 40, p. 175–191.

White, N.C., and Hedenquist, J.W., 1990, Epithermal environments and styles of mineralization: variations and their causes, and guidelines for exploration: in Hedenquist, J.W., White, N.C., and Siddeley, G., eds., *Epithermal Gold Mineralization of the Circum-Pacific; Geology, Geochemistry, Origin and Exploration*, II, 36(1-3): *Journal of Geochemical Exploration*, Elsevier, Amsterdam, p. 445–474.

White, N.C., and Hedenquist, J.W., 1995, Epithermal gold deposits: styles, characteristics and exploration: *SEG Newsletter*, v. 23, p. 9–13.

Wilson, J. J., 1983. Cretaceous stratigraphy of the central Andes of Peru, *Bulletin of the American Association of Petroleum Geology*, v. 47, p. 1-34.

Wilson, J. J., 2000. Structural development of the northern Andes of Peru, X Congress of Peruvian Geology, Lima, 2000.

## **28 CERTIFICATE OF QUALIFIED PERSON: Derrick Strickland**

I, Derrick Strickland, do hereby certify as follows:

I am a consulting geologist at 1251 Cardero Street, Vancouver, B.C.

This certificate applies to the technical report entitled "NI43-101 Technical Report on the Pucarini Property, in Distrito de Palca, Provincia de Lampa, Departamento de Puno. Juliaca, in Peru 15°55'56"S 70°30'51"W" with an effective and signature date of February 15, 2021

I am a graduate of Concordia University of Montreal, Quebec, with a B.Sc. in Geology, 1993. I am a Practicing Member in good standing of the Association of Professional Engineers and Geoscientists, British Columbia, license number 278779, since 2003. I have been practicing my profession continuously since 1993 and have been working in mineral exploration since 1986 in gold, precious, base metal, and coal mineral exploration. During which time I have used, applied geophysics/ geochemistry, across multiple deposit types. I have worked throughout Canada, United States, China, Mongolia, South America, South East Asia, Ireland, West Africa, Jamaica, Papua New Guinea, and Pakistan.

I have read the definition of "qualified person" set out in National Instrument 43-101 ("NI 43-101") and certify that by reason of my education, affiliation with a professional organization (as defined in NI 43-101) and past relevant work experience, I fulfill the requirements to be a "qualified person" for the purposes of NI 43-101.

I am responsible sections 1 to 5, 6, 9, 11, 13 to 27 and have read all sections of the report entitled "NI43-101 Technical Report on the Pucarini Property, in Distrito de Palca, Provincia de Lampa, Departamento de Puno. Juliaca, in Peru 15°55'56"S 70°30'51"W with an effective and signature date of February 15, 2021.

I have not visited the Pucarini Property the subject of this report

I am independent of Forte Minerals Corp., Globetrotters Resources Peru SAC, and Cordillera Resources SAC as defined by applying the tests in section 1.5 of National Instrument 43-101. I am not, nor have been, an officer, director, or employee of any corporate entity that is any part of the subject Pucarini Property. For greater clarity, I do not hold, nor do I expect to receive, any securities or any other interest in any corporate entity, private or public, with interests in the Pucarini Property or to receive any other consideration besides fair remuneration for the preparation of this report. I have not earned the majority of my income during the preceding three years from any corporate entity, private or public, with interests in the Pucarini Property.

I have had no prior involvement with the Pucarini Property that is the subject of this Technical Report.

I have read National Instrument 43-101, Form 43-101F1, and confirm that the portions of the technical report for which I am responsible have been prepared in compliance with that Instrument.

I certify that, to the best of my knowledge, information and belief, that, as of the Effective Date, the portions of the Technical Report for which I am responsible contain all the scientific and technical information that is required to be disclosed to make this technical report not misleading.

The "NI43-101 Technical Report on the Pucarini Property, in Distrito de Palca, Provincia de Lampa, Departamento de Puno. Juliaca, in Peru 15°55'56"S 70°30'51"W effective and signature date of February 15, 2021

### **"Original Signed and Sealed"**

On this day 15 February 2021  
Derrick Strickland P. Geo.

## **CERTIFICATE OF QUALIFIED PERSON: Steven Park**

I, Steven L. Park, do hereby certify as follows:

I am a consulting geologist residing at 19505 Sedgefield Terrace, Boca Raton, Florida, USA.

This certificate applies to the report entitled "NI43-101 Technical Report on the Pucarini Property, in Distrito de Palca, Provincia de Lampa, Departamento de Puno. Juliaca, in Peru 15°55'56"S 70°30'51"W" with an effective and signature date of February 15, 2021

I am a graduate of Mackay School of Mines at the University of Nevada-Reno, 1983, with a M.Sc. in Economic Geology. I have since practiced as a professional geologist for more than thirty years in the Americas including over 20 years of continuous exploration experience in Peru evaluating and managing mineral exploration programs covering a variety of mineral deposit types. I am a member in good standing with the American Institute of Professional Geologists (member #10849) and a Certified Professional Geologist.

I have read the definition of "qualified person" as defined by National Instrument 43-101 and certify that by reason of my education, past relevant work experience, and professional affiliation, I fulfill the requirements to be a "qualified person" for the purposes of NI 43-101

I am responsible for Sections 7, 8, 10, and 12 of this technical report and have read all sections of the report entitled "NI43-101 Technical Report on the Pucarini Property, in Distrito de Palca, Provincia de Lampa, Departamento de Puno. Juliaca, in Peru 15°55'56"S 70°30'51"W with an effective and signature date of February 15, 2021.

I visited the Pucarini Property, subject of this technical report, on November 22, 2020.

I am independent of Forte Minerals Corp., Globetrotters Resources Peru S.A.C. and Cordillera Resources SAC as defined by applying the tests set out in Section 1.5 of the Instrument. I am not, nor have been, an officer, director, or employee of any corporate entity that is any part of the subject Pucarini Property. For greater clarity, I do not hold, nor do I expect to receive any securities or any other interest in any corporate entity, private or public, with interests in the Pucarini Property or to receive any other consideration besides fair remuneration for the preparation of this report. I have not earned the majority of my income during the preceding three years from any corporate entity, private or public, with interests in the Pucarini Property.

I have had no prior involvement with the Pucarini Property that is the subject of this technical report.

I have read National Instrument 43-101, Form 43-101F1, and confirm that the portions of the technical report for which I am responsible have been prepared in compliance with that Instrument.

I certify that, to the best of my knowledge, information and belief, that, as of the Effective Date, the portions of the Technical Report for which I am responsible contain all the scientific and technical information that is required to be disclosed to make this technical report not misleading.

The "NI43-101 Technical Report on the Pucarini Property, in Distrito de Palca, Provincia de Lampa, Departamento de Puno. Juliaca, in Peru 15°55'56"S 70°30'51"W effective and signature date of February 15 2021

"Original Signed and Sealed"

Steven L. Park

On this 15th day of February 2021